SHEAR VISCOSITY BEHAVIOR NEAR THE DOUBLE CRITICAL POINT OF THE MIXTURE 3-METHYLPYRIDINE, WATER AND HEAVY WATER

by

GEOFFRY ALAN LARSEN

B.S., Southwest Texas State University, 1981

A MASTER'S THESIS

submitted in partial fulfillment of the

requirements for the degree

MASTER OF SCIENCE

Department of Physics

KANSAS STATE UNIVERSITY

Manhattan, Kansas

1984

Approved by:

Christopher M Sorensen

Major Professor

TABLE OF CONTENTS

LIST OF FIGURES

Figure Page

LIST OF TABLES

Table | Page

ACKNOWLEDGEMENTS

This thesis is dedicated to my mother, Mary Patricia Larsen. While she did not live to see it completed, I could never have gotten this far without her support and love.

I would like to thank both my father, Pernell Larsen, Sr., and my wife, Lew. My father was always there with his advice and help. If I am half the man he is when I reach his age, I will have achieved something in this world. Lew, my wife, was always there with her love and encouragement. She waited many times for me to come home from the lab late into the night, but always was patient with me.

I would also like to thank Chris Sorensen, my major professor. Not only was he patient with me and supportive, but he taught me two important attitudes. First, always try to look at things as simply as you can. Second, do things one step at a time. It was always a pleasure to work with him and I learned volumes just watching him think about problems.

Special thanks go to Dave Hill and Bob Geering. Without the fellows in the machine shop, none of us would ever get anything done. Their knowledge, experience, and willingness to help make them invaluable to this department.

I also would like to thank KoKo Himes. She typed the manuscript for me and shepherded me through the process of meeting all of my deadlines.

Lastly, I would like to thank Dave Hare for the help he gave me when I was calibrating the viscometers and measuring solution densities.

Chapter I

INTRODUCTION

The behavior of fluid systems in the vicinity of a critical point is a topic that has been studied with great interest throughout this century. In particular, interest has been focused on critical point exponents since the middle of this century.

Most of the systems studied have been systems that are miscible at higher temperatures, but which unmix over a range of concentrations as the temperature is lowered below an upper critical temperature. For binary fluid systems, it has been found that the critical exponents take on universal values. That is, they do not depend on the specific system being studied. Furthermore, theories have been developed that have predicted with success the values taken on by these exponents. For example, the shear viscosity critical exponent of binary fluids has been predicted to have a value of about 0.040 using both mode-mode coupling theory and renormalization group theory. Experimental tests of this prediction have tended to support it, although there have been exceptions. For examples of experimentally determined values for the shear viscosity critical exponent, ϕ, see Table I.

In more recent years, theoreticians and experimentalists have become more interested in systems that display reentrant behavior. These solutions, usually mixtures of hydrogen bonding liquids, remix when the temperature is lowered still further below a lower critical solution temperature. In Fig. 1, we see a coexistence surface for such a liquid. Some quite satisfactory

TABLE I

Shear Viscosity Critical Exponents of Various Solutions

System	ϕ	Comments
Water/Ethanol/Chloroform	0.054[b]	Analysis of data from Ref. j)
	0.052[b]	Analysis of data from Ref. j)
	0.042[j]	
2.6-Lutidine/Water	0.038[a]	Analysis of data from Ref. g)
	0.041[b]	Analysis of data from Ref. g)
	0.043[b]	Analysis of data from Ref. h)
	0.039[c]	Analysis of data from Ref. h)
3-Methylpyridine/Nitroethane	0.035[a]	Analysis of data from Ref. d)
	0.040[b]	Analysis of data from Ref. d)
	0.038[b]	Analysis of data from Ref. d)
	0.038[b]	Analysis of data from Ref. d)
	0.038[b]	Analysis of data from Ref. e)
	0.040[c]	Analysis of data from Ref. e)
	0.039[c]	Analysis of data from Ref. d)
	0.039[e]	
Isobutyric Acid/Water	0.038[a]	Analysis of data from Ref. f)
	0.029[b]	Analysis of data from Ref. f)
	0.039[c]	Analysis of data from Ref. f)
Aniline/Cyclohexane	0.033[b]	Analysis of data from Ref. i)

a) T. Ohta, J. Phys. C 10 (1977) 791.
b) S. P. Lee, Chem. Phys. Lett. 57 (1978) 611
c) P. Calmettes, Phys. Rev. Lett. 39 (1977) 1151
d) A. Stein, J. C. Allegra and G. F. Allen, J. Chem. Phys. 56 (1971) 4265.
e) B. C. Tsai and D. McIntyre, J. Chem. Phys. 60 (1974) 937.
f) J. C. Allegra, A. Stein and G. F. Allen, J. Chem. Phys. 55 (1971) 1716.
g) E. Gulari, A. F. Collings, R. L. Schmidt and C. J. Pings, J. Chem. Phys. 56 (1972) 6169.
h) A. Stein, S. J. Davidson, J. C. Allegra and G. F. Allen, J. Chem. Phys. 56 (1972) 6164.
i) C. C. Yang and F. R. Meeks, J. Phys. Chem. 75 (1971) 2619.
j) S. P. Lee and A. J. Purvis, Chem. Phys. 24 (1977) 191.

Figure 1. This figure shows the general appearance of the miscibility dome for the H_2O/D_2O/3-methylpyridine system. Notice for mixtures rich in D_2O and weak in H_2O that the coexistance curve is a simple closed loop with separate upper and lower critical points that are single critical points. As the concentration of H_2O is increased, the loop shrinks until the upper and lower critical points merge, becoming a double critical point. The mixtures we are interested in are those in the immediate vicinity of the double critical point.

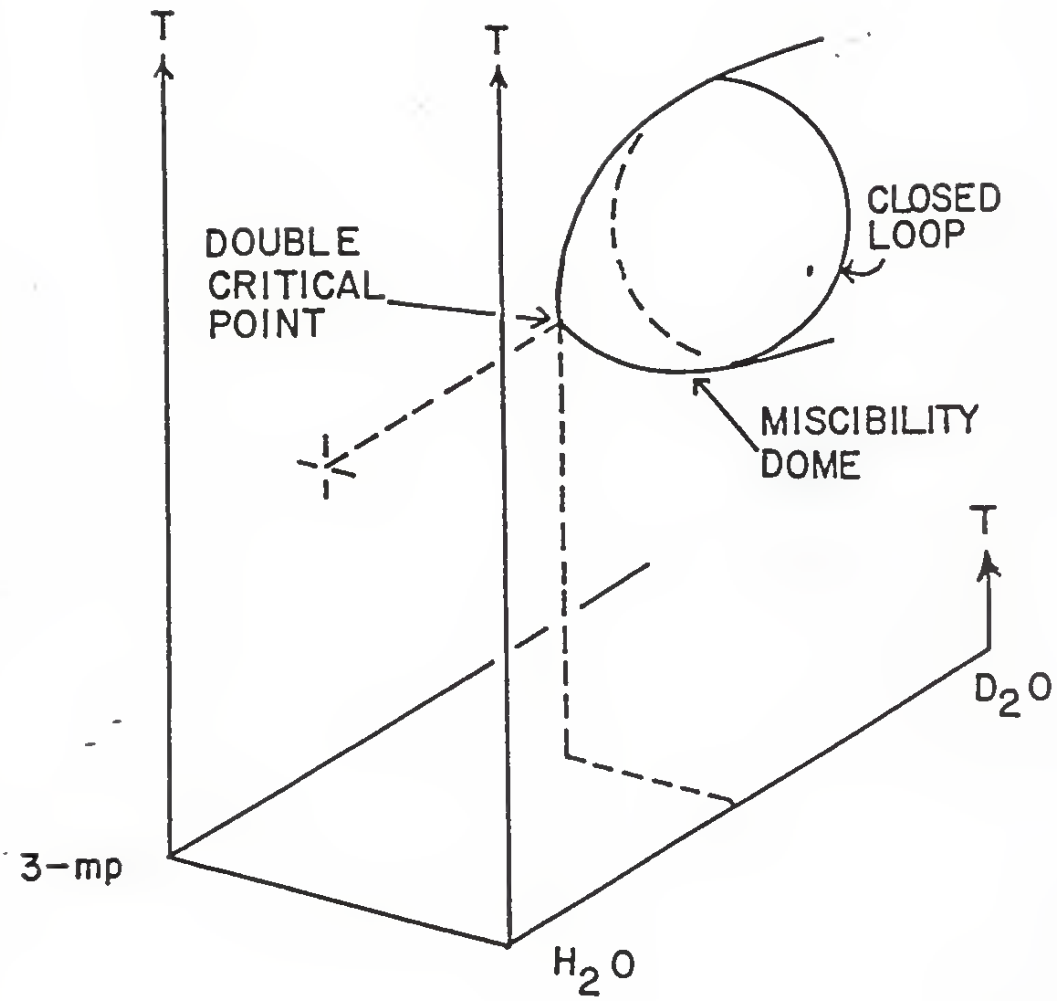
T
T
CLOSED
LOOP
DOUBLE
CRITICAL
POINT
MISCIBILITY
DOME
T
D_2O
3-mp
H_2O

theories have been developed to account for this behavior.[1,2] In these theories, the specific orientational nature of hydrogen bonding has been presented as the reason why these liquids could remix at lower temperatures and still have a monotonically decreasing entropy.[3]

Consider Fig. 1, beginning with the closed loop. The upper- and lowermost points on this loop represent an upper critical solution point and lower critical solution point, respectively. If the 3-methylpyridine concentration is held fixed while the ratio of H_2O to D_2O is increased, the two critical points begin to approach each other as the loop closes. Eventually, they come together to form what is called a double critical point. One result that has come out of the study of these systems has been that the critical exponents are predicted to double as the double critical point is approached.[1-4] In these theories, it is pointed out that, if the double critical point is approached tangentially (see Fig. 2), the path followed as the critical temperature, T_c, is approached comes much closer to points on the critical surface than to the double critical point itself. Each point on the critical surface is an Ising critical point. The parameter determining the separation of the system from criticality when on this tangential path should actually be the distance from the closest point on the critical surface. In the laboratory, we would measure the temperature deviation from criticality as ε where

$$\varepsilon = |T-T_{DCP}|/T_{DCP}$$

and T_{DCP} is the temperature at the double critical point. As can be seen in Fig. 2, the parabolic shape of the critical surface leads us to conclude that this deviation should actually be ε^2. This is the source of the prediction that the critical exponent should double.

Figure 2. In this figure, we can see the rationale behind the prediction that the critical exponents will double as the double critical point is approached. Here, the solid line represents the critical points for different concentrations of the H_2O/D_2O/3-methylpyridine system. As we progress from 0 to 1 on the abscissa-axis, H_2O is substituted for D_2O in the system. 0 indicates no H_2O in the system, while 1 indicates no D_2O. The dashed line represents the path taken as we fix the concentration at the double critical point concentration and vary the temperature. Notice as we approach P that we are much closer to P' than to P. This is the basis for the idea that, as the double critical point concentration is approached, the critical phenomena anomalies will vary as ε^{2x} rather than ε^{x}.

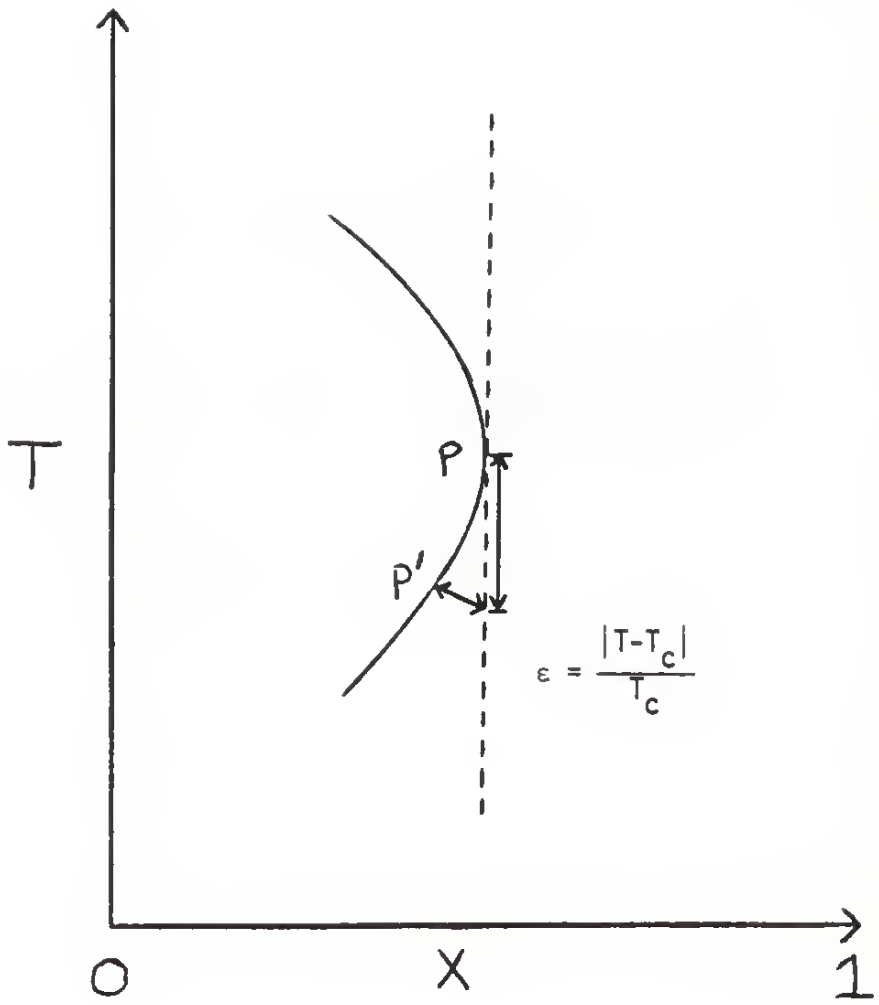
T
P
P'
$\varepsilon = \frac{|T-T_c|}{T_c}$
0
X
1

While these predictions have been tested with success on a gas-gas[5] and a liquid-crystal[6] system, no published results exist for a binary fluid system. The purpose of this experiment was to find evidence to support or reject the hypothesis that the shear viscosity critical exponent, ϕ, should double as the double critical point was approached.

The system studied in this experiment was actually a ternary mixture of H_2O, D_2O, and 3-methylpyridine that was initially examined by Cox and Andon[7] in a series of papers in the 1950's. For the characteristics of this system, see Fig. 3.

While this is not a true binary system, we feel that this system can be characterized as quasi-binary because of its unique composition. This concept has been tried before with success by Gulari et al.[8] and Knobler and Scott[9] on ternary systems of deuterated or non-deuterated mixtures of isobutyric acid and water. These systems displayed binary solution behavior in the one phase region. In addition, Goldstein[2] has successfully treated mixtures of H_2O with 2,6-dimethylpyridine and one of the monomethyl pyridines as a quasi-binary system. The substitution of H_2O for D_2O should not affect the properties of the system except insofar as the strength of the hydrogen bonding is weakened. The result is that the mixture of D_2O and H_2O can be treated as one liquid whose hydrogen bond strength is, on the average, a compositionally weighted average of the D_2O and H_2O hydrogen bond strengths. Therefore, we feel that the behavior of the shear viscosity in this mixture of H_2O, D_2O, and 3-methylpyridine should mirror that of a true binary system.

Two methods of analyzing the data will be used. These will be referred to as the Ohta analysis and Kortan analysis.

In the Ohta analysis, the viscosity data will be examined in the manner suggested by T. Ohta in a paper published in 1976.[10] Prior to this time,

Figure 3. Shown are two cross-sections of the miscibility dome for the H_2O/D_2O/3-methylpyridine system. In the upper figure, $W_{H_2O}=0$ where W is weight-percent concentration. W_{D_2O} and $W_{3\text{-MP}}$ are varied. In the lower figure, $W_{3\text{-MP}}=0.30$. W_{H_2O} and W_{D_2O} are varied.

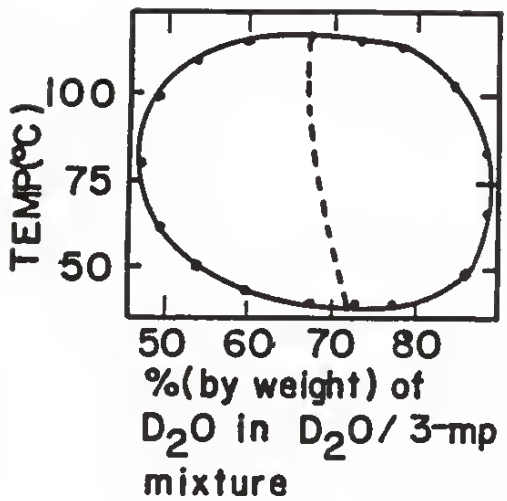
TEMP(°C)
100
75
50
50 60 70 80
%(by weight) of
D_2O in D_2O/ 3-mp
mixture

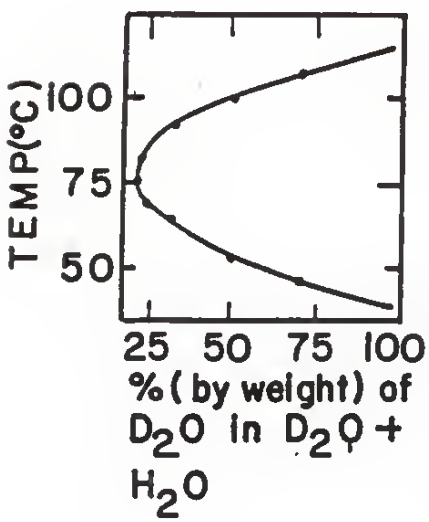
TEMP(°C)
100
75
50
25 50 75 100
%(by weight) of
D_2O in D_2O +
H_2O

the shear viscosity anomaly had been treated as additive in nature. In other words,

$$\eta(T) = \eta_0(T) + \Delta\eta(T) \tag{1-1}$$

and the background viscosity, $\eta_0(T)$, would be subtracted from the actual viscosity, $\eta(T)$, to find the size of the anomaly. However, in this paper, Ohta found better agreement with experiments if the anomaly was treated as being multiplicative in nature. In other words, the correct expression was

$$\eta(T) = \eta_0(T)\varepsilon^{-\phi} \tag{1-2}$$

where ϕ is the shear viscosity critical exponent. Note then that

$$\eta(T)/\eta_0(T) = \varepsilon^{-\phi} \ . \tag{1-3}$$

We are interested in the behavior of the ratio $\eta(T)/\eta_0(T)$ as T_c is approached.

The Kortan analysis involves two phenomological expressions developed empirically by Kortan et al. in a paper published in 1983.[6] In this experiment, reentrant behavior in a liquid crystal was studied. For concentrations exhibiting a phase transition between nematic and smectic-A phases, the correlation lengths were described by

$$\xi = \xi^0[\varepsilon + (T_c/\Delta T)\varepsilon^2]^{-\nu} \tag{1-4}$$

where ξ^0 is a concentration dependent parameter and ΔT is the separation between upper and lower critical solution temperatures, UCST and LCST.

If the concentration was such that there was no phase transition, the correlation lengths were described by

$$\xi = A[(T-T_m)^2 + a(y-y_0)]^{-\nu} \tag{1-5}$$

where A and a are constants, y_o is the double critical point concentration, T_m is the temperature at the center of the coexistance loop, and y is the concentration of the solution.

As can be seen in the first expression, if the loop is large, the first term is dominant and the correlation lengths goes as $\varepsilon^{-\nu}$. On the other hand, if ΔT gets small enough, then the second term dominates and the correlation length goes as $\varepsilon^{-2\nu}$. As such, we see critical exponent doubling. In the second expression, we see that the correlation length should go as $(T-T_m)^{-2\nu}$.

Chapter II

EXPERIMENTAL PROCEDURE

Solution Preparation

The D_2O used in this experiment was purchased from Alfa Products. The lot analysis printed on the bottle stated the fluid to be at least 99.8% D_2O.

Doubly distilled water was obtained from within the department. The first distillation was through a charcoal filter unit. The second was through an ion exchange unit.

Our 3-methylpyridine was purchased from Aldrich. It was technical grade and was yellow in color. We cleaned a fractional distillation unit, flushed it twice, and oven-dried it. The 3-methylpyridine was then distilled twice, the middle half being kept each time. The boiling point of 3-methylpyridine is 144.1^{o}C. During distillation, the column temperature varied between 143^{o}C and 144^{o}C. After distillation, the distillate was colorless. The final distillate was stored in a clean, oven-dried, brown chemical bottle which had a teflon seal in the cap. In addition the cap was sealed with parafilm.

We saved the first and fourth quarters from the second distillation process. Some of this distillate was poured into two distillation flasks. These flasks were glass stoppered and sealed with parafilm. In addition, one of the two flasks was wrapped in aluminum foil to exclude light. After several months, there was still no sign of discoloration that might indicate decomposition. We saw no change in either of these samples over the duration of the experiment.

The rest of the first and fourth quarters was distilled a third time.

The two middle quarters of the resulting distillate were again saved. During this time the column temperature varied between 143°C and 160°C. This was an indication that the distillate contained other methylpyridines and dimethylpyridines since these have higher boiling points than 3-methylpyridine. We stored the distillate in a clean, oven-dried, brown chemical bottle as before. Again, the cap had a teflon seal inside, and the cap itself was sealed with parafilm.

Stock solutions of H_2O/3-methylpyridine and D_2O/3-methylpyridine were mixed under dry nitrogen such that the weight percentage of 3-methylpyridine in each was 29.9%±0.1%. This ensured both ease in mixing and that any samples made would have the same weight-percentage of 3-methylpyridine. The stock solutions were mixed up using volumetric pipettes. Densities for D_2O, H_2O, and 3-methylpyridine were taken from values given in the 1976-77 edition of the CRC Handbook of Chemistry and Physics. The stock solutions were also stored in clean, oven-dried, brown chemical bottles with teflon seals in the caps.

All of our chemicals were stored at all times under dry nitrogen gas in a glove box that also contained $CaSO_4$ as a dessicant. This ensured the absence of any atmospheric water in our storage area.

All of the samples were mixed inside the glove box using volumetric pipettes. They were stored in 10 milliliter vials that had teflon seals in the lids. The pipettes and vials were carefully cleaned with distilled water and acetone, flushed with distilled water, and oven-dried prior to their use. The samples were stored in the glove box.

Determination of the Critical Concentration

From prior work done by Cox,[7] we knew that the concentration of 3-methyl pyridine at the tip of the miscibility dome was close to 30 weight-%. This

number was not exact, since Cox was not really concerned with that. This was why the stock solutions were mixed as they were. The first step in finding the critical concentration was to find the proportion of D_2O to H_2O such that phase separation no longer occurred. Once this was accomplished, we were able to increase the D_2O concentration by very small amounts and have upper and lower critical solution temperatures that were only three to five degrees apart. Because both stock solutions were mixed at the same weight percentage of 3-methylpyridine, the 3-methylpyridine's concentration did not change as the D_2O/H_2O concentration was varied.

After this was done, we varied the 3-methylpyridine concentration and watched to see what happened to the volume ratio of the two fluids above and below the meniscus, while holding the temperature fixed as close to the phase separation temperature as possible. If, on a given trial, the 3-methylpyridine concentration was along the critical isochore, the ratio should be one. If the 3-methylpyridine concentration was slightly off of the isochore, then one of the two phase would disappear as the lower critical temperature was approached from above. With the correct concentrations of 3-methylpyridine, H_2O , and D_2O, both the upper and lower phases would disappear simultaneously as the lower critical temperature was approached. We started with a known volume of a sample in the viscometer and added small amounts of 3-methylpyridine as the ratio of the upper to lower volumes was observed. A typical sample size was 4 milliliters, and the sample concentration was shifted in 0.1 to 0.25 mole-% increments. A volumetric micropipette was used to shift the 3-methylpyridine concentration in each sample.

Best results were obtained when $X_{H_2O} = 0.7880$, $X_{D_2O} = 0.1290$, and $X_{3\text{-MP}} = 0.0830$. For this concentration, a $0.05^{o}C$ shift in temperature from the one-phase region to the two-phase region resulted in a ratio between

the lower and upper volumes of one to two.

Viscosity Measurement and Temperature Control

Viscosity was determined by measuring capillary flowtimes. The viscometer consists of a long, narrow capillary with a dumping reservoir on one end and a sample chamber on the other end (see Fig. 4). The sample chamber has three ports. One leads to the capillary; another leads to a fill reservoir from which the sample chamber is filled; and the third is a vent. In addition, the dumping reservoir, fill reservoir, and vent are all joined by a piece of tubing. This allows the viscometer to be completely immersed in a temperature-controlled water bath and also enables us to refill the sample chamber by simply rotating the viscometer. The viscometer is made of glass.

Sealing the viscometer was difficult. The viscometer was filled through a port in the dumping reservoir, which was plugged after filling. The plug had to be made of a material inert to 3-methylpyridine. We took a piece of teflon and inserted it into a clear glass vial containing 3-methylpyridine. After a week had passed, the fluid was still clear and colorless, and the teflon appeared unchanged. So, we first tried making teflon plugs.

We found we were unable to provide a good seal with these plugs for two reasons. The first was that the diameter of the inner wall of the port lip was smaller than that of the inner wall of the port just past the lip. If a plug could get by the lip, then it was too small to seal effectively against the inner wall of the port. The second problem was that, after cycling the temperature two or three times, the plug would take a set. In other words, it would lose its ability to return to its former dimensions.

We solved both of these problems by modifying the plug. We drilled a hole through the plug into which we could insert a stainless steel bolt. We then drilled and threaded a hole about halfway through a

Figure 4. Shown is a diagram of the viscometer and the plug. The viscometer is made from glass. The sample chamber is filled from the fill reservoir. Flow-times are timed with the viscometer vertical and the fill reservoir on top. The stopwatch is started when the upper meniscus passes through the vent and stopped when the upper meniscus exits the bottom of the sample chamber where the capillary begins.

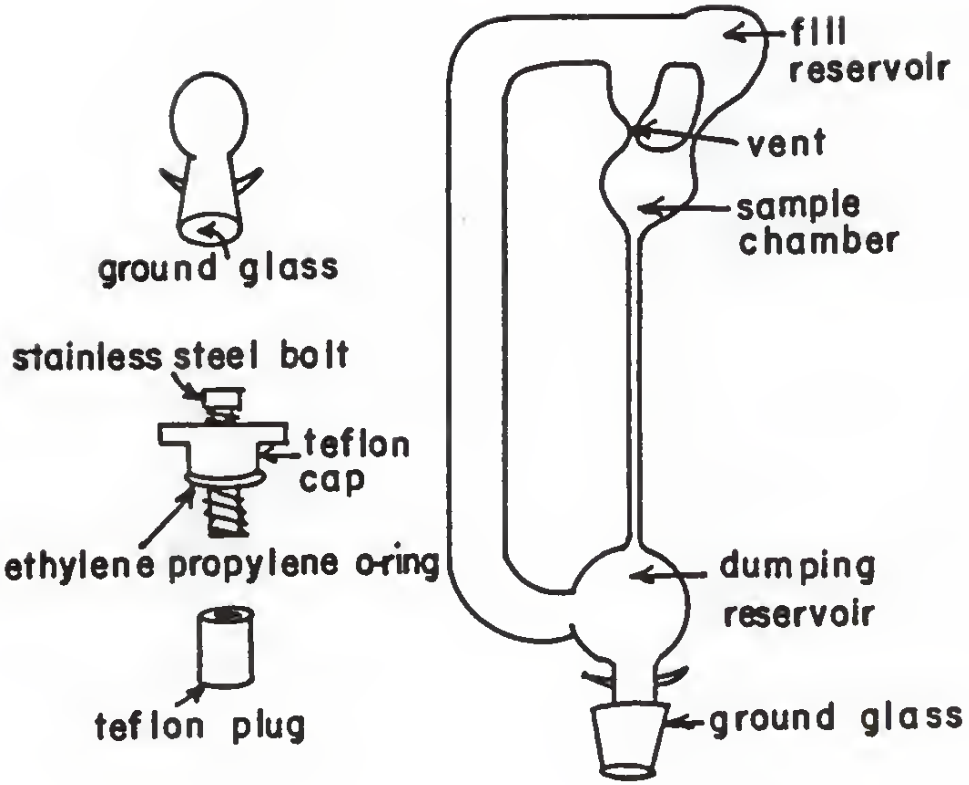
fill reservoir
vent
sample chamber
ground glass
stainless steel bolt
teflon cap
ethylene propylene o-ring
dumping reservoir
teflon plug
ground glass

second piece of teflon. We then screwed the bolt through the plug, slipped on an ethylene propylene O-ring, and screwed the bolt into the second piece of teflon. By turning the bolt clockwise, we compressed the O-ring between the two pieces of teflon. Screwing the bolt counter-clockwise let the O-ring relax. In this manner we could slip the plug into the viscometer and then compress the O-ring. This squeezed the O-ring against the inner wall and provided a good seal.

In choosing ethylene propylene for the O-ring material, we searched technical literature to see what materials were suggested for this purpose. We then tested an ethylene propylene O-ring in the same manner in which we tested the teflon. The results, as before, indicated no effect.

In addition to modifying the plug, we modified the port so that it had a ground glass exterior and a matching ground glass cap. With the aid of a little vacuum grease, this provided a second seal. Two spikes each were added to both the cap and port, so that the cap could be secured with rubber bands.

Prior to loading with a sample, the viscometer was cleaned in the following manner. The viscometer was first flushed several times with distilled water, then once or twice with spec grade acetone. After this, the viscometer was again flushed several times with distilled water. No detergent was used in the cleaning process for two reasons. The first was that we used distilled water and 3-methylpyridine and very pure D_2O. Since the pipettes used to load the viscometer were themselves carefully cleaned and dried prior to use, there should have been no foreign material present to require the use of soap. The second reason was the obvious difficulty of flushing the capillary and the fill tube completely of soap. The viscometer plug was cleaned in the same manner.

After this, the viscometer was oven-dried to remove any water or

acetone left. The plug was air-dried and then placed in the glove box. After removing the viscometer from the oven, it too was placed in the glove box. As mentioned before, the inside of the glove box continuously had both a dessicant present and dry nitrogen gas flowing through.

The viscometer was loaded in the glove box with pipettes that had been cleaned and dried with the viscometer. A typical sample volume was 4 milliliters. After loading the viscometer, it was mounted on a stand on which the viscometer was free to rotate. The entire apparatus was placed in a temperature-controlled water bath.

The viscometer was first rotated so that the liquid gathered in the fill reservoir. The viscometer was then slowly rotated to allow the sample chamber to fill from the fill reservoir, while air in the sample chamber escaped through the vent. After the sample chamber was filled, the viscometer was rotated so that the capillary was vertical. The time necessary for the sample chamber to empty was recorded with a hand held stopwatch to 0.01 seconds. By again rotating the viscometer, the sample was transferred from the dumping reservoir to the fill reservoir. The process could then be repeated.

We used three separate viscometers during the course of the experiment. It was necessary to determine the viscometer constant, K, for each viscometer as a function of temperature. To do so, we took doubly distilled water and measured its capillary flowtime in each viscometer every ten degrees over the entire temperature range of the experiment. We took the density and viscosity values from tables in the 1976-77 edition of the CRC Handbook. Then, for each temperature, T, we have

$$K(T) = \eta/Dt \qquad (2\text{-}1)$$

To determine the density of each solution over the experiment's temperature range, we used 2 milliliter and 5 milliliter pycnometers. We

determined the density every ten to fifteen degrees for five different concentrations until the fluid separated each time. We used a Mettler balance to determine the solution mass at each temperature. We used interpolation to determine the densities for other concentrations.

Temperature control was achieved by placing the viscometer into a large insulated water bath. We achieved fine temperature control using a Neslab Exocal 30000 water bath externally to control the viscometer bath temperature to $\pm 0.1^{o}C$ for temperatures below $80^{o}C$. When the temperature exceeded $80^{o}C$, temperature control was $\pm 0.2^{o}C$. In addition, we used a YSI Model 72 controller, when we made temperature changes, to speed up the process.

Chapter III

OHTA ANALYSIS

As explained in the introduction, an expression for the behavior of the viscosity of a solution near a critical point is

$$\eta(T) = \eta_0(T)\varepsilon^{-\phi} \qquad (3\text{-}1)$$

where $\eta_0(T)$ is the background viscosity, ϕ is the critical exponent and

$$\varepsilon = |T-T_c|/T_c \quad .$$

Rewriting the expression and taking the logarithm of both sides, Eq. (3-1) becomes

$$\log[\eta(T)/\eta_0(T)] = -\phi \log \varepsilon \qquad (3\text{-}2)$$

This suggests that as a method of determining ϕ, we may graph $\log[\eta(T)/\eta_0(T)]$ versus $\log \varepsilon$. With the appropriate choice of T_c, the result is a straight line with slope $-\phi$. Given the data for $\eta(T)$, we need $\eta_0(T)$ and T_c before performing our analysis.

Determining $\eta_0(T)$ was definitely the most difficult task in this analysis. This would not have been the case if, in the critical regime, the actual viscosity had become much greater than the background viscosity. If this had occurred, then a small error in the determined value of $\eta_0(T)$ would not have had a noticeable effect on the function of interest, $\eta(T)/\eta_0(T)$. However, the actual viscosity never exceeded the background viscosity by more than about 26 percent. Much more precision in temperature control would have been

necessary before we could have observed $\eta(T)$ become much larger than $\eta_0(T)$. As such, great care needed to be taken in determining $\eta_0(T)$.

The first approach tried was the standard one of looking at data sufficiently far from the critical point that the viscosity anomaly was negligible, and trying to fit it to a modified Arrhenius equation of the form

$$\eta(T) = A \exp[B/(T-T_0)] \qquad (3\text{-}3)$$

where A, B, and T_0 are constants. In our analysis, we determined the range of temperatures over which the viscosity anomaly could be considered negligible by considering the behavior of χ^2, a measure of the goodness of our fit, as data from temperatures successively closer to the phase separation temperature were included in our fit to Eq. (3-3). As long as the viscosity anomaly remained negligible, χ^2 was not noticeably affected by the addition of temperatures closer to the phase separation temperature. When the anomaly was no longer negligible, the modified Arrenhius equation was no longer sufficient to describe the viscosity data and χ^2 increased.

As an example, consider the H_2O/3-methylpyridine solution. For this sample, $X_{H_2O} = 0.9238$, $X_{D_2O} = 0.0000$, and $X_{3\text{-mp}} = 0.0762$. This solution did not phase-separate. First, the points from 10.05°C to 30.00°C were fit to Eq. (3-3). Then, more points were successively included in the fit and the resultant χ^2 for the fit was observed. In this example, the final fit was determined over the temperature range from 10.05°C to 35.00°C. The results are shown in Table II. Note how quickly χ^2 begins to increase when data points for temperatures greater than 35.00°C are included in the fit.

An alternative method of determining the background viscosity occurred to us when we examined Fig. 5. In this figure, flowtime is plotted versus temperature for several different solutions. Note that the curves tend to

Table II. This table lists the results of a chi-square fit of the shear viscosity measurements of H_2O/3-methylpyridine to Eq. (3-3). These fits were performed on a computer. σ was entered as 1%. The equation being fit is

$$\eta(T) = B \exp\left(\frac{A}{T-T_o}\right).$$

TABLE II

Number of Points	Temperature Range (^{o}C)	B(cp)	A(^{o}K)	T_o(^{o}K)	χ^2
5	10.05-30.00	.02899	586.0	158.1	.703
6	10.05-35.00	.02950	587.4	157.3	.770
7	10.05-40.00	.03075	581.9	157.2	1.008
8	10.05-45.05	.03125	582.2	156.6	1.039
10	10.05-55.00	.03297	579.1	155.6	1.847

Figure 5. Viscometer flowtime is plotted versus temperature for four representative solutions. The first two listed below phase separated and the other two did not phase separate.

△ X_{H_2O}=0.3914 X_{D_2O}=0.5279 $X_{3\text{-MP}}$=0.0807

○ X_{H_2O}=0.7880 X_{D_2O}=0.1290 $X_{3\text{-MP}}$=0.0830

□ X_{H_2O}=0.8020 X_{D_2O}=0.1207 $X_{3\text{-MP}}$=0.0772

◇ X_{H_2O}=0.9238 X_{D_2O}=0.0000 $X_{3\text{-MP}}$=0.0762

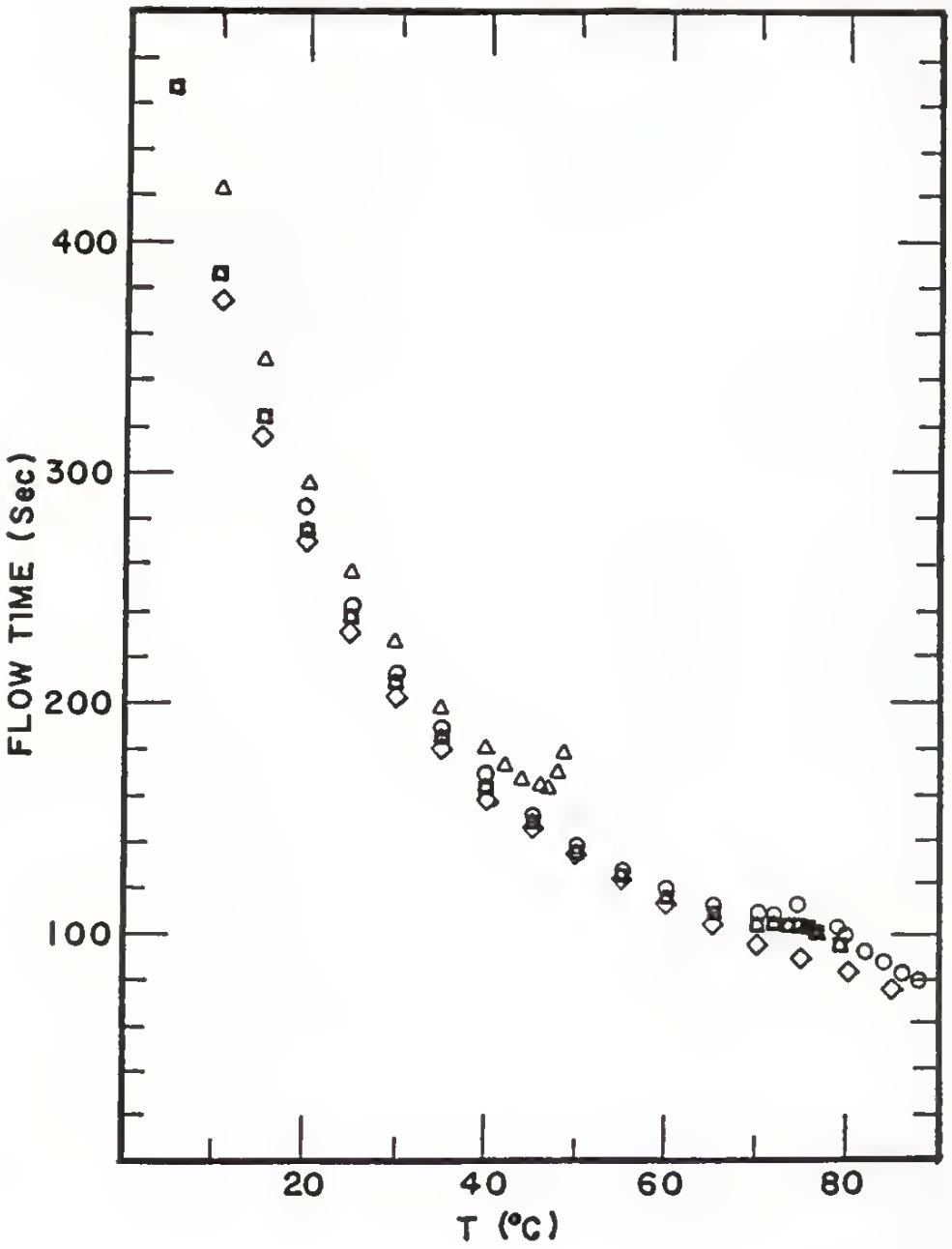
FLOW TIME (Sec)
400
300
200
100
20
40
60
80
T (°C)

lie on top of each other when far from the critical temperatures. This led us to consider the possibility of the background viscosity for a given concentration being directly proportional to the background viscosity for H_2O/3-methylpyridine, which seemed to exhibit only a small anomaly. This approach has been used successfully before.[11] Given that the 3-methylpyridine concentration varied so little in all of our mixtures and given the similarities between D_2O and H_2O, this seemed to be a reasonable system on which to try this approach.

To test this idea, we decided to normalize $\eta(T)$ by $\eta_B(T)$ for each solution and each temperature, T. $\eta_B(T)$ is the background viscosity of H_2O/3-methylpyridine that we determined using the χ^2 test.

In Figures 6 and 7, $\eta(T)/\eta_B(T)$ is plotted versus temperature for the separating and non-separating solutions, respectively. Note how the individual curves flatten as we get sufficiently far from the phase separation temperatures for the separating solutions. The same thing occurs for non-separating solutions when far enough from T_{DCP}, the double critical point temperature. This seems to support the idea that the background viscosity for each solution was a multiple of the background viscosity of H_2O/3-methylpyridine.

For each concentration, the ratio of $\eta(T)/\eta_B(T)$ was determined by averaging the values from the flat portions of the curves in Figs. 6 and 7. The resultant ratios are plotted versus concentration in Fig. 8. Mixtures for which viscosity measurements were not done over a large enough temperature range to see this flattening were excluded. Note the linear nature of this curve. The background viscosity for each solution was determined

Figure 6. In this figure, the ratio η/η_B is plotted versus temperature for the concentrations, given below, that phase separated. η is the experimentally measured viscosity for each mixture. η_B is the background viscosity for H_2O/3-methylpyridine.

◇ $X_{H_2O}=0.0000$ $X_{D_2O}=0.9160$ $X_{3\text{-MP}}=0.0840$

△ $X_{H_2O}=0.3914$ $X_{D_2O}=0.5279$ $X_{3\text{-MP}}=0.0807$

⬡ $X_{H_2O}=0.7356$ $X_{O_2O}=0.1866$ $X_{3\text{-MP}}=0.0778$

□ $X_{H_2O}=0.7926$ $X_{D_2O}=0.1298$ $X_{3\text{-MP}}=0.0776$

○ $X_{H_2O}=0.7880$ $X_{O_2O}=0.1290$ $X_{3\text{-MP}}=0.0830$

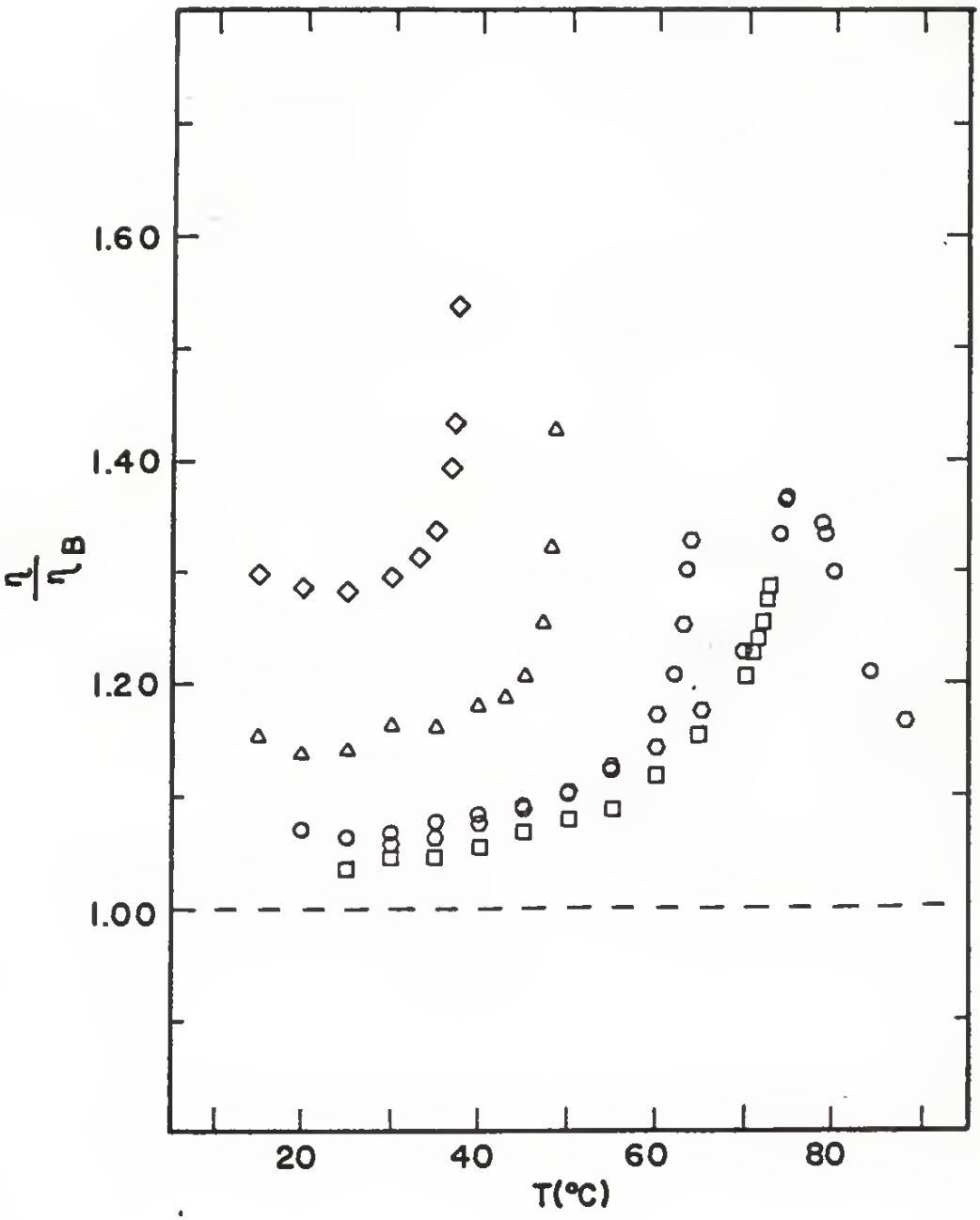
1.60
1.40
1.20
1.00
$\frac{\eta}{\eta_B}$
20
40
60
80
T(°C)

Figure 7. In this figure, the ratio η/η_B is plotted versus temperature for the concentrations, given below, that did not phase separate. η is the experimentally measured viscosity for each mixture. η_B is the background viscosity for H_2O/3-methylpyridine.

△ X_{H_2O}=0.7954 X_{D_2O}=0.1245 $X_{3\text{-MP}}$=0.0801

○ X_{H_2O}=0.7987 X_{D_2O}=0.1241 $X_{3\text{-MP}}$=0.0773

□ X_{H_2O}=0.8020 X_{D_2O}=0.1207 $X_{3\text{-MP}}$=0.0772

⬡ X_{H_2O}=0.8061 X_{D_2O}=0.1165 $X_{3\text{-MP}}$=0.0774

◇ X_{H_2O}=0.9238 X_{D_2O}=0.0000 $X_{3\text{-MP}}$=0.0762

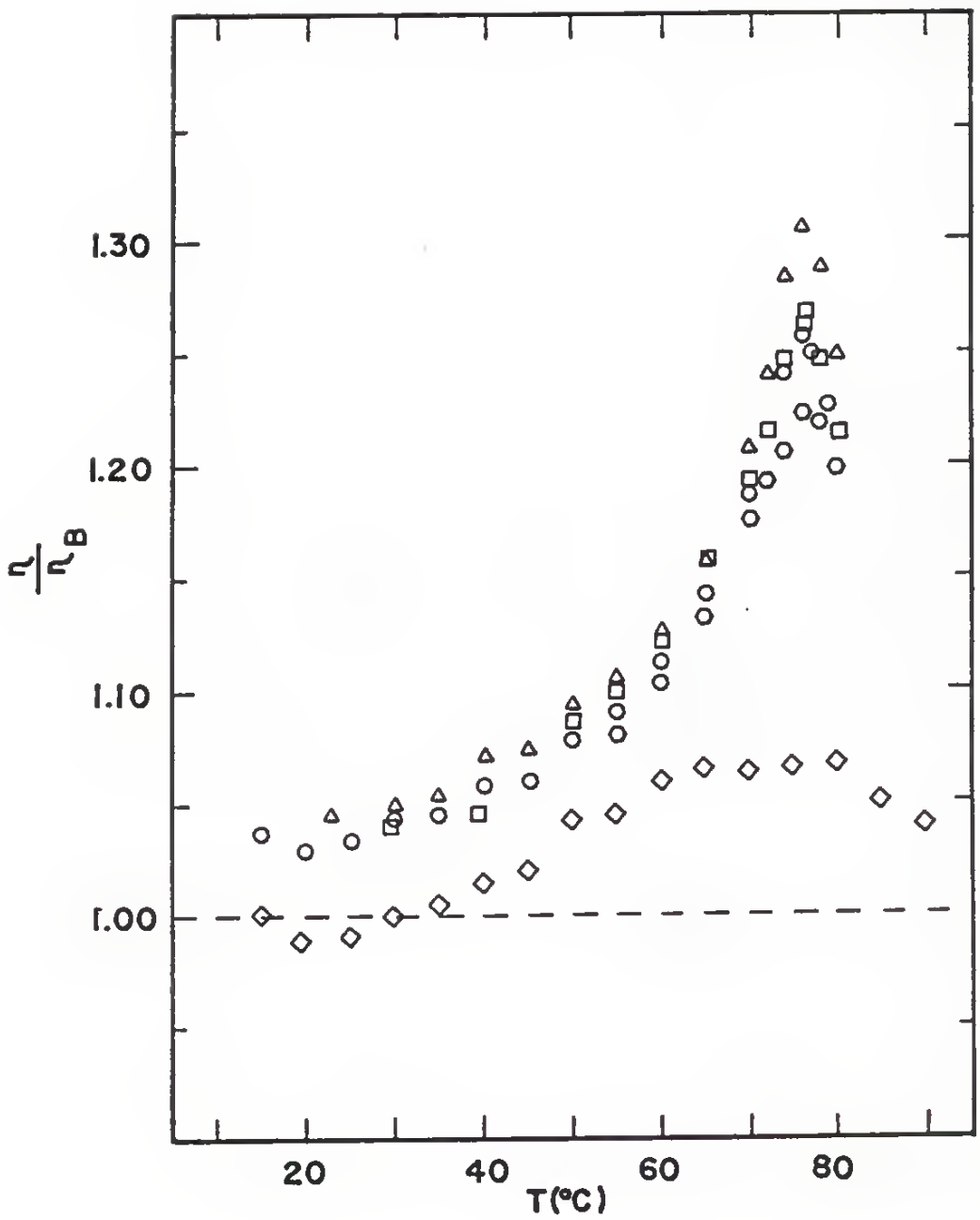
1.30
1.20
1.10
1.00
η/η_B
20
40
60
80
T(°C)

Figure 8. In this figure, the ratio η_o/η_B is plotted versus V for eight concentrations. η_o is the background viscosity for each mixture. η_B is the background viscosity for H_2O/3-methylpyridine. V is the ratio of the volume of D_2O to the volume of (D_2O+H_2O) for each solution when they were mixed. Note that η_o/η_B is fairly linear with respect to V.

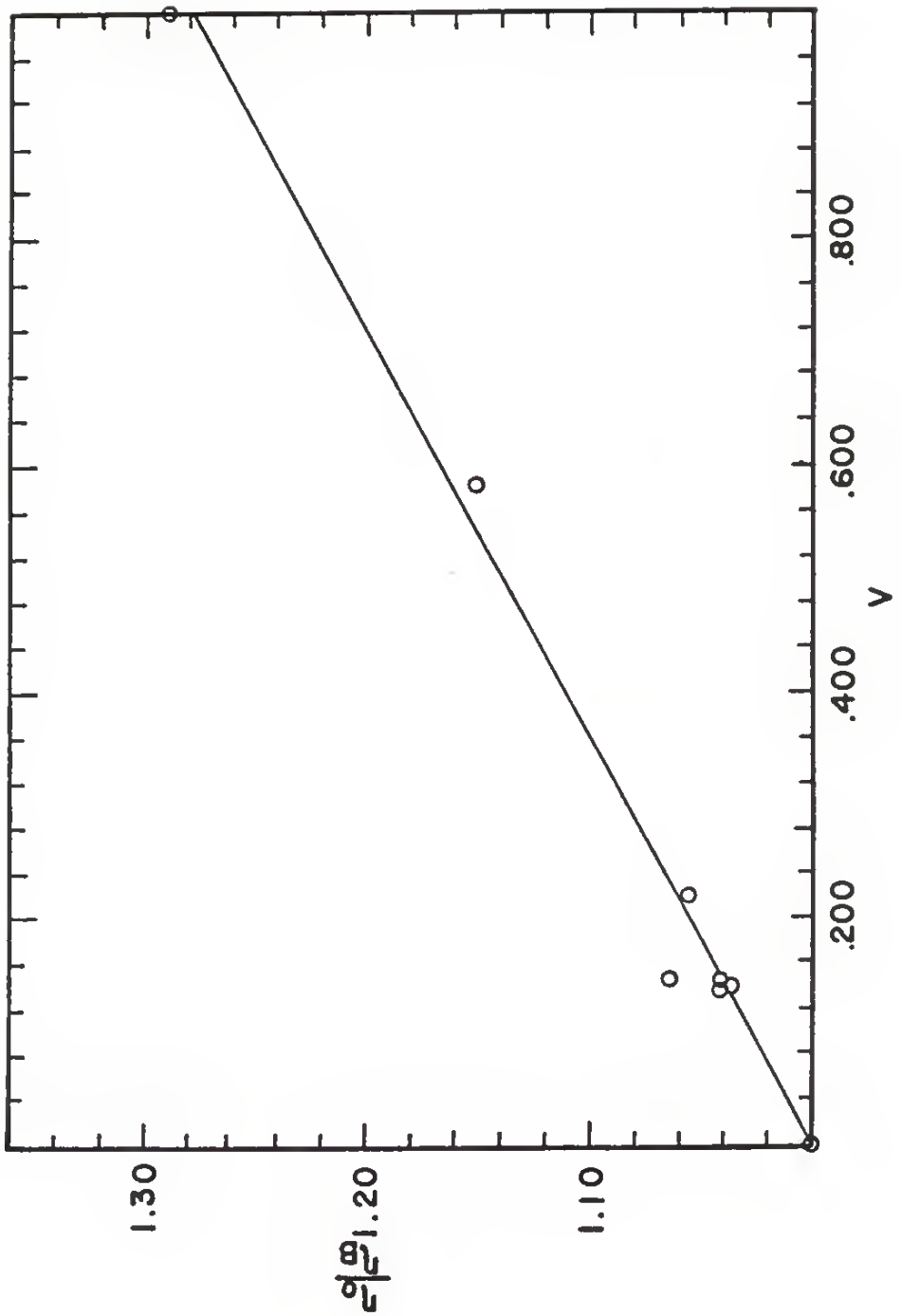
1.30
1.20
1.10
.200
.400
.600
.800
V

by multiplying $\eta_B(T)$ by the corresponding ratio for that solution. For solutions for which a value of the ratio could not be determined from the raw data, the value was taken from the curve in Fig. 8.

We are now left only with determining T_c, the critical temperature, for each mixture. How can this be done? For any solution mixed along the critical concentration isochore, the critical temperature is identical to the phase separation temperature. However, it was very difficult to mix our solutions so that they were on the critical isochore since we did not know the correct critical concentration. What happens to the relationship between the critical temperature and phase separation temperature when we are off the critical isochore?

The answer depends on the size and shape of the miscibility loop as well as the degree to which we lie off of the critical isochore. If we are close enough to the critical isochore, the critical temperature will still be very nearly equal to the phase separation temperature. A larger loop with the miscibility curve somewhat flatter along the bottom results in an increase in the region on either side of the critical isochore in which the critical temperature is still very nearly equal to the phase separation temperature. As we progress further from the critical isochore, the difference between the two temperatures increases.

The "critical temperature" for a concentration off of the critical isochore is actually an effective critical temperature and is referred to as a spinodal temperature.[12-15] Like the critical temperature for a solution on the critical isochore, an effective critical temperature is the temperature at which a singularity exists for the solution in question. Unlike a solution on the critical isochore, a region of metastability exists between the phase separation temperature and the effective critical temperature. These

spinodal temperatures are said to lie along a spinodal curve, or spinodal. In addition, a spinodal loop is always smaller than the corresponding miscibility loop. To avoid confusion, these effective critical temperatures will simply be referred to as critical temperatures in this paper.

How then was the critical temperature determined for a solution which did not lie along the critical isochore? The value of T_c was chosen such that the graph of $\log[\eta(T)/\eta_0(T)]$ versus $\log \varepsilon$ was best linearized. It was assumed that shear thinning was not involved. In addition, if viscosity data were available for temperatures above the upper critical temperature, an attempt was made to symmetrize the results for temperatures above and below the upper and lower critical temperatures, respectively.

When we say the results were symmetrized, we mean the following. Consider a solution with a closed coexistence curve, in other words one with both upper and lower critical solution temperatures, UCST and LCST. Now, simultaneously consider two identical samples. The first sample is at a temperature $T_1 \ll$ LCST and the second $T_2 \gg$ UCST such that $(\text{LCST} - T_1)/\text{LCST} = (T_2 - \text{UCST})/\text{UCST} = \varepsilon$ and ε is large enough that $\log \varepsilon \approx 0$. Then, $\eta(T)/\eta_0(T) \simeq 1$ for both T_1 and T_2. Furthermore, $\eta(T_1)/\eta_0(T_1) = \eta(T_2)/\eta_0(T_2)$ since $\eta(T)/\eta_0(T)$ is only a function of ε. Now, slowly increase T_1 and slowly decrease T_2 so that the condition $(\text{LCST} - T_1)/\text{LCST} = (T_2 - \text{LCST})/\text{UCST}$ is retained. What do we notice about $\eta(T_1)/\eta_0(T_1)$ and $\eta(T_2)/\eta_0(T_2)$? They will remain equal to each other. This is what we mean when we say the results are symmetrized. As long as $(\text{LCST} - T_1)/\text{LCST} = (T_2 - \text{UCST})/\text{UCST}$, $\eta(T_1)/\eta_0(T_1) = \eta(T_2)/\eta_0(T_2)$.

So, there are two tests that can be used to see if the correct upper and lower critical temperatures have been determined. The first is that the curve $\log \eta(T)/\eta_0(T)$ versus $\log \varepsilon$ be a straight line. The second is that

$\eta(T_1)/\eta_o(T_1) = \eta(T_2)/\eta_o(T_2)$, as long as $(LCST - T_1)/LCST = (T_2 - LCST)/UCST$, what we call a symmetry in ε. Both of these tests were taken into account when determining the critical temperature for a given solution.

For concentrations which did not unmix, those beyond the double critical point, symmetrization weighed more heavily than linearization. As can be seen for such a solution in Fig. 16, a value for T_c cannot be chosen to perfectly linearize the entire curve. There is not a critical point for such a mixture and we expect Eq. (3-2) to fail to describe such a system. At some point for each solution beyond the double critical point, $\eta(T)/\eta_o(T)$ ceased to increase and leveled off until we were past T_{DCP}, the double critical point temperature. Then, it would begin to decrease. If ε is defined here as $|T-T_{DCP}|/T_{DCP}$, the curve is symmetrical in ε as before. This might be described in terms of a virtual, or imaginary, critical point. In such a description, the virtual critical point would be a projection of the double critical point into composition-temperature space beyond the miscibility dome. The behavior of the viscosity anomaly as a virtual critical point was approached could be described empirically by the expression

$$\log \eta(T)/\eta_o(T) = -\phi H[\varepsilon-\varepsilon_o(X_{DCP}-X)]\log \varepsilon - \phi(1-H[\varepsilon-\varepsilon_o(X_{DCP}-X)])\log\varepsilon_o(X_{DCP}-X) \qquad (3\text{-}4)$$

where

$$H[\varepsilon-\varepsilon_o(X_{DCP}-X)] = \begin{cases} 1 & \varepsilon>\varepsilon_o \\ 0 & \varepsilon\leq\varepsilon_o \end{cases}$$

$\varepsilon_o(X_{DCP}-X)$ obviously is equal to the value of ε at which the curve $\log \eta(T)/\eta_o(T)$ versus $\log \varepsilon$ levels off. Note that $\varepsilon_o(X_{DCP}-X)$ goes to zero as X goes to X_{DCP}. At the double critical point itself, $\log[\eta(T)/\eta_o(T)]$

is infinite in value when $T = T_{DCP}$ and $X = X_{DCP}$.

Now that the background viscosities and critical temperatures were known for each solution, $\log[\eta(T)/\eta_0(T)]$ was plotted versus $\log \varepsilon$ for each one and the graphs are shown in Figs. 9 through 21. The slopes, and hence the critical exponents, are tabulated in Table III.

The double critical point concentration itself was never found. However, from our observations of the relative volumes of the upper and lower solutions at T_{sep} for various solutions, we can say that it is in the immediate vicinity of $X_{H_2O} = 0.788$, $X_{D_2O} = 0.127$, and $X_{3\text{-mp}} = 0.085$.

The first conclusion that can be drawn from Table III is that the critical exponent definitely increased as the double critical point was approached. Notice that ϕ increased from 0.038 for D_2O/3-methylpyridine to 0.072 for the solution closest to the double critical point. The value of ϕ for D_2O/3-methylpyridine is somewhat less than the theoretical value of 0.041; but, as seen in Table I which lists a variety of previous experimental results, this is not an unusual occurrence.

The second conclusion that can be drawn from Table III is that the exponent increase did not become strong until we were within about 1 mole percent of the correct H_2O concentration at the double critical point. Here, the exponent appears to increase rapidly.

Beyond the double critical point, the shear viscosity behavior was similar to that of the separating mixtures with some differences. When far from T_{DCP}, we found that $\log[\eta(T)/\eta_0(T)]$ versus $\log \varepsilon$ could be both linearized and symmetrized. ε for non-separating solutions is defined to be

$$\varepsilon = |T-T_{DCP}|/T_{DCP} \quad .$$

Figure 9. On a log-log scale, η/η_o is plotted versus ε. For this mixture, X_{H_2O}=0.000, X_{D_2O}=0.9160, and $X_{3\text{-MP}}$= 0.0840. The line has a slope of -0.038. The LCST is 37.35^{o}C.

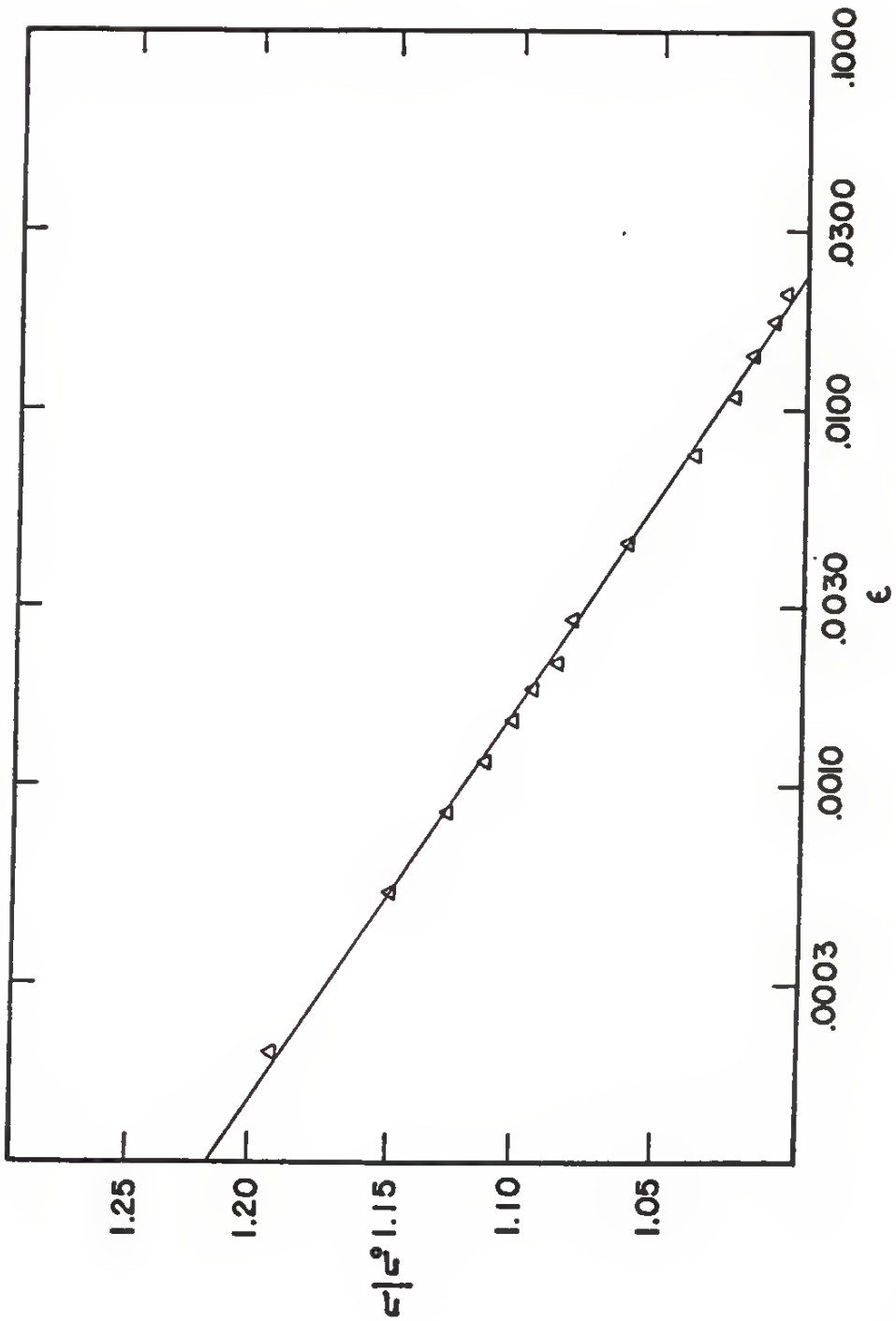
1.25
1.20
1.15
1.10
1.05
$\epsilon = |\epsilon|^{\beta}$
.0003
.0010
.0030
.0100
.0300
.1000
ϵ

Figure 10. On a log-log scale, η/η_o is plotted versus ε. For this mixture, X_{H_2O}=0.3914, X_{D_2O}=0.5279, and $X_{3\text{-MP}}$= 0.0807. The line has a slope of -0.050. The LCST is 48.50°C.

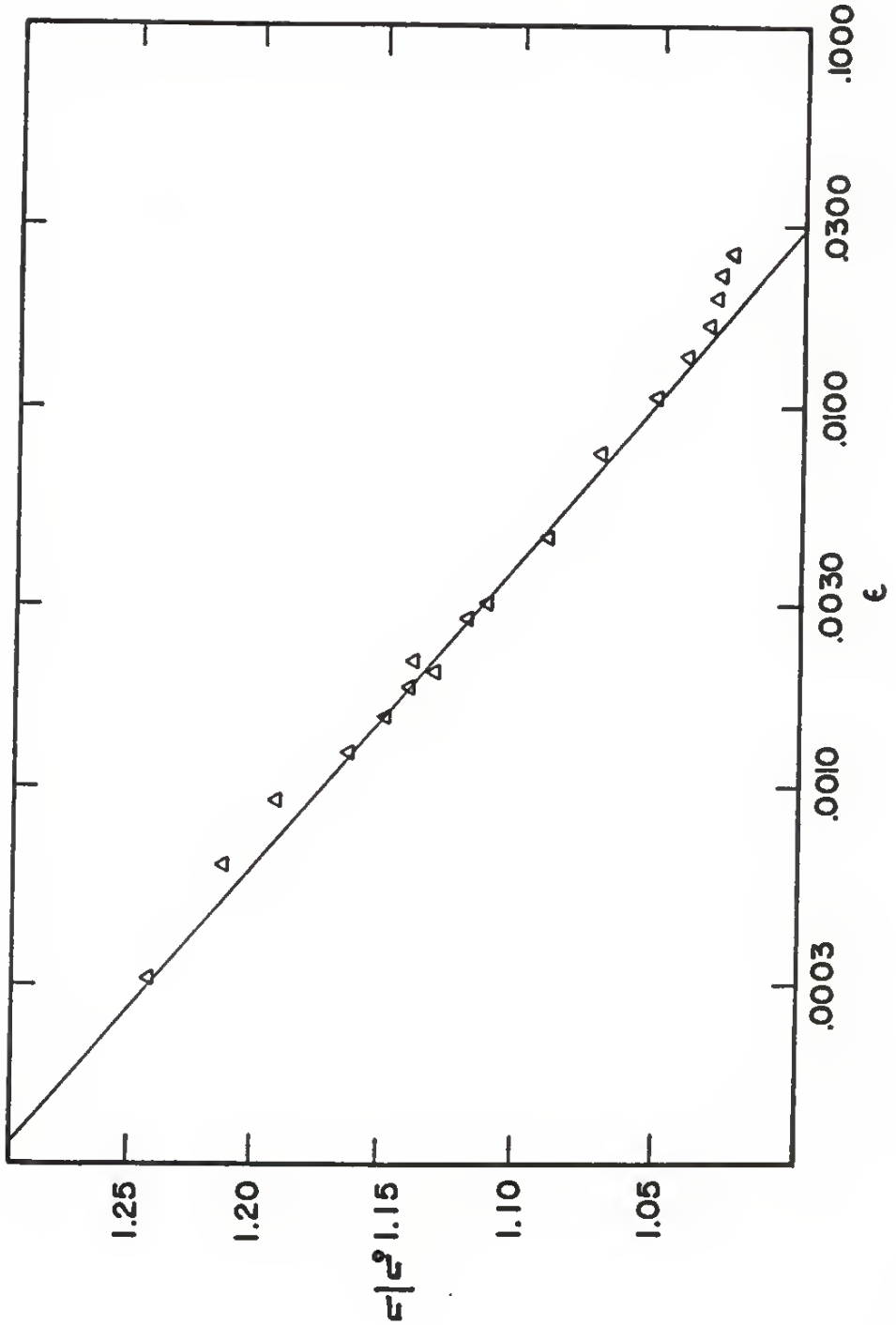
1.25
1.20
1.15
1.10
1.05
$\tau = |\epsilon|^{2\beta}$
.0003
.0010
.0030
.0100
.0300
.1000
ϵ

Figure 11. On a log-log scale, η/η_o is plotted versus ε. For this mixture, X_{H_2O}=0.7356, X_{D_2O}=0.1866, and $X_{3\text{-MP}}$= 0.0778. The line has a slope of -0.051. The LCST is 64.00°C.

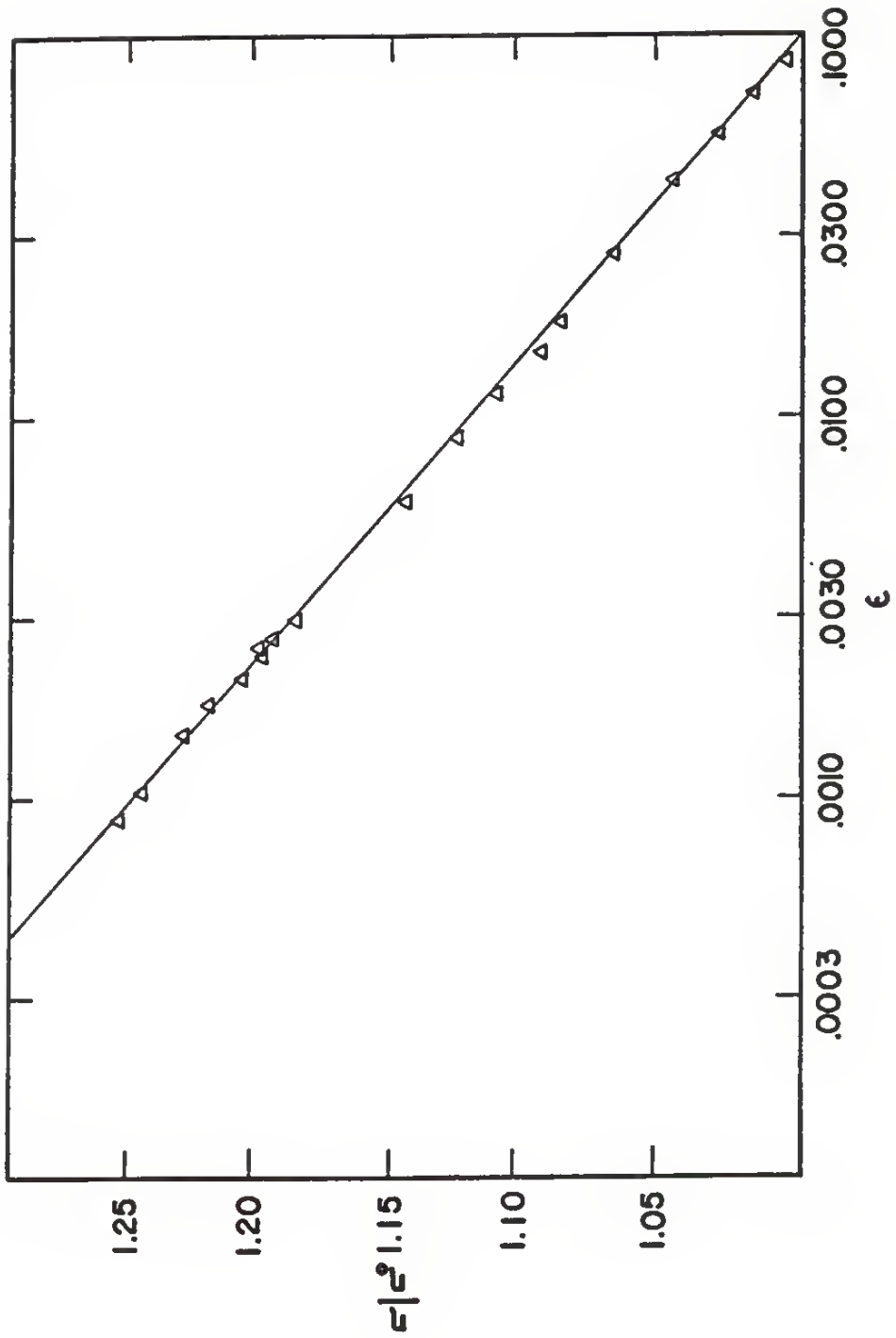
1.25
1.20
1.15
1.10
1.05
τ/τ^0
.0003
.0010
.0030
.0100
.0300
.1000
ϵ

Figure 12. On a log-log scale, η/η_0 is plotted versus ε. For this mixture, X_{H_2O}=0.7926, X_{O_2O}=0.1298, and $X_{3\text{-MP}}$= 0.0776. The line has a slope of -0.064. The LCST is 74.00°C.

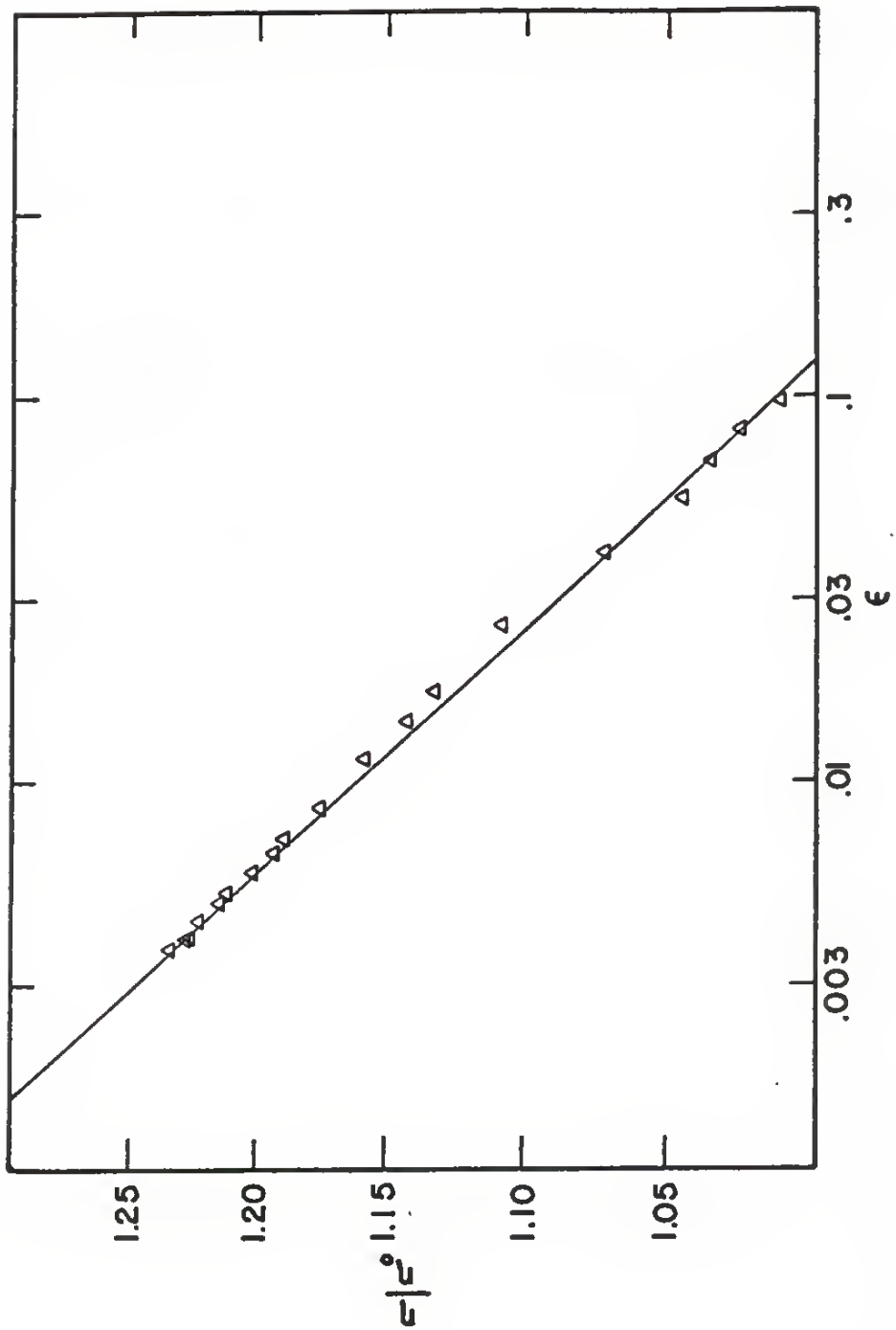
1.25
1.20
1.15
1.10
1.05
$\tau = |t|^{2\beta}$
.3
.1
.03
.01
.003
ϵ

Figure 13. On a log-log scale, η/η_o is plotted versus ε. For this mixture, X_{H_2O}=0.7880, X_{D_2O}=0.1290, and $X_{3\text{-MP}}$= 0.0830. The line has a slope of -0.072. The LCST 75.50°C and the UCST is 77.50°C.

△ T < LCST

▽ T > UCST

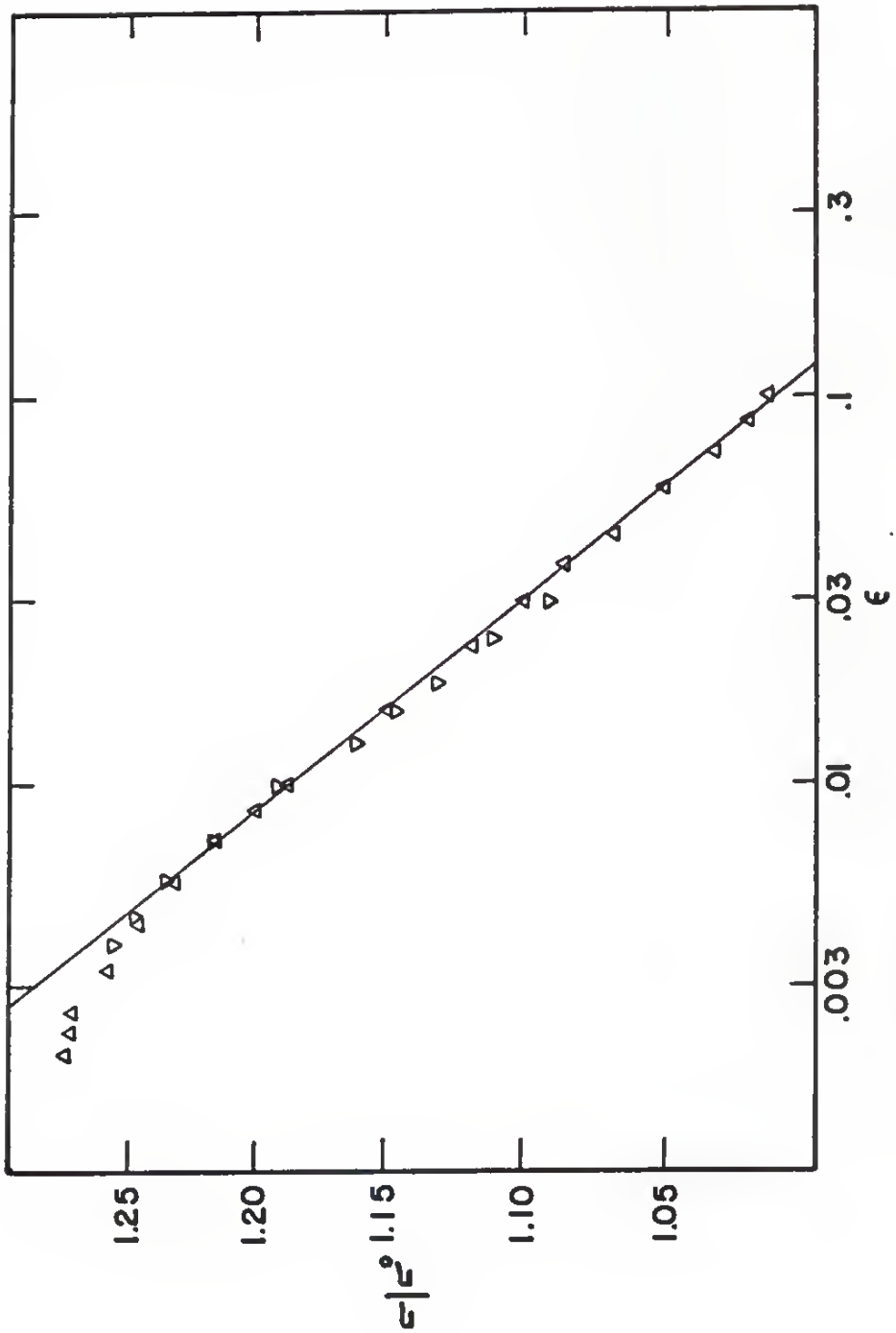
1.25
1.20
1.15
1.10
1.05
τ/τ_c^0
.003
.01
.03
.1
.3
ϵ

Figure 14. In a log-log scale, η/η_0 is plotted versus ε for the solution shown in Fig. 13. In this figure, however, we have LCST=UCST=76.4°C. Notice that the figure is somewhat less symmetric. In addition, the graph has acquired an s-shape in its appearance. From this we can see the necessity of using both the tests of linearity and symmetrization in determining the upper and lower critical solution temperatures.

△ $T < 76.4^{o}C$

▽ $T > 76.4^{o}C$

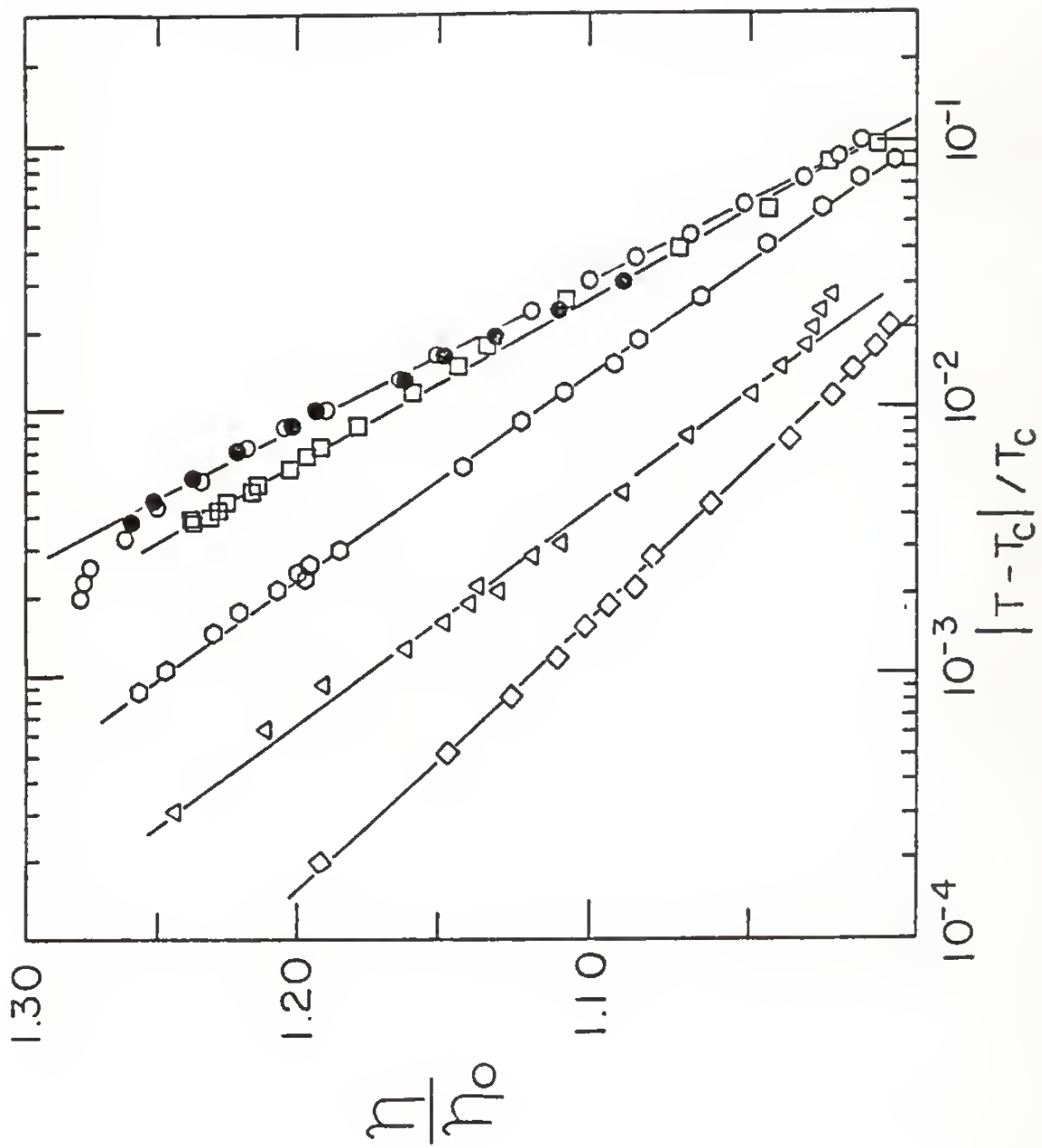
1.30
1.20
1.10
η/η0
10^-1
10^-2
10^-3
10^-4
|T - Tc| / Tc

Figure 15. Shown is a composite of Figs. 9-13. We can easily see the increase in the slope of the lines, and hence the shear viscosity critical exponents, as the double critical point concentration is approached. In addition, note that the anomaly becomes visible much sooner as we approach the double critical point concentration.

◇ $X_{H_2O}=0.0000$ $X_{D_2O}=0.9160$ $X_{3\text{-MP}}=0.0840$

△ $X_{H_2O}=0.3914$ $X_{D_2O}=0.5279$ $X_{3\text{-MP}}=0.0807$

⬡ $X_{H_2O}=0.7356$ $X_{D_2O}=0.1866$ $X_{3\text{-MP}}=0.0778$

□ $X_{H_2O}=0.7926$ $X_{D_2O}=0.1298$ $X_{3\text{-MP}}=0.0776$

○ (T < LCST) $X_{H_2O}=0.7880$ $X_{D_2O}=0.1290$

● (T > USCT) $X_{3\text{-MP}}=0.0830$

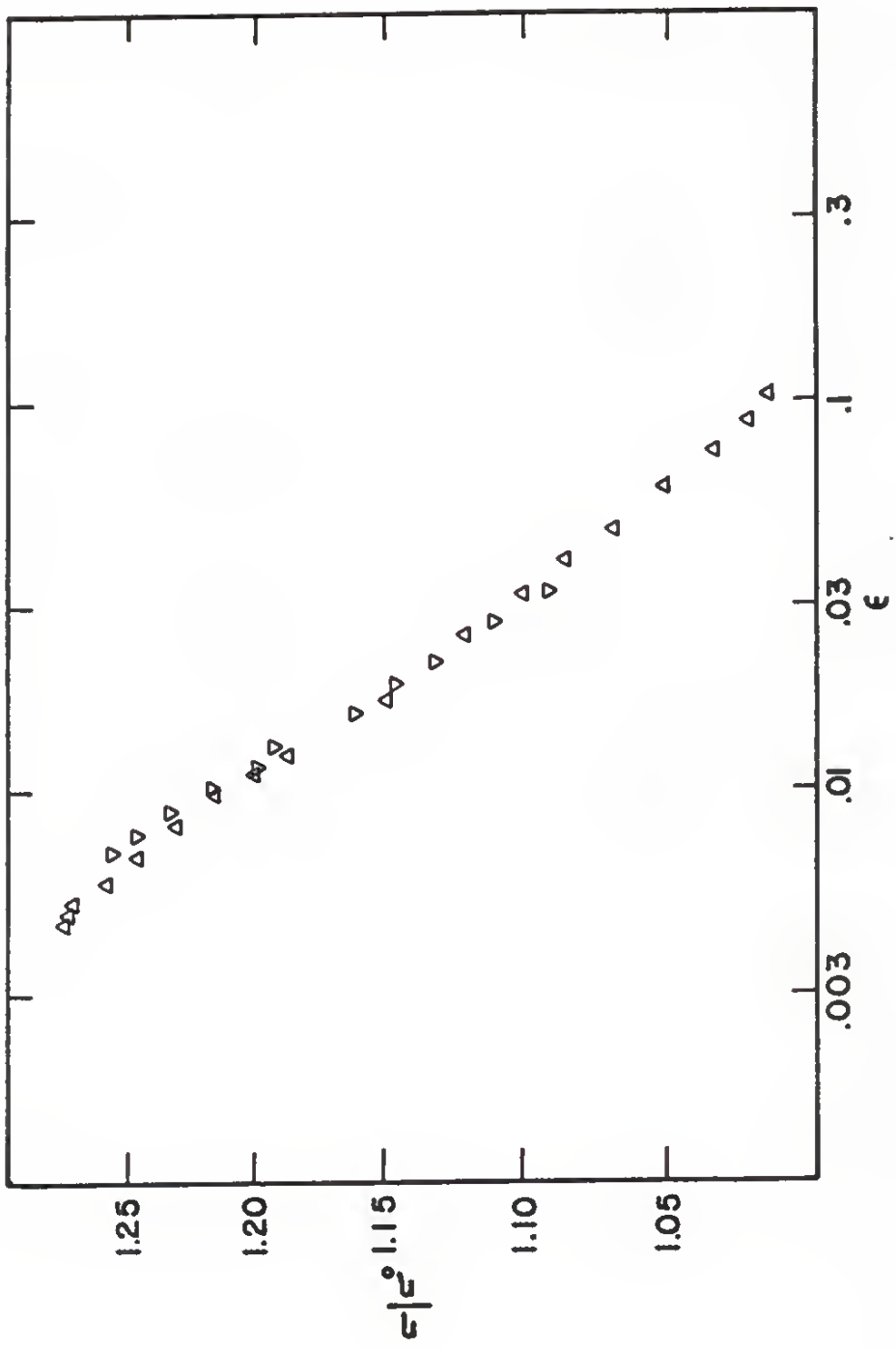
1.25
1.20
1.15
1.10
1.05
τ/τ_c
.003
.01
.03
.1
.3
ϵ

Figure 16. On a log-log scale, η/η_o is plotted versus ε. For this mixture, X_{H_2O}=0.7954, X_{D_2O}=0.1245, and $X_{3\text{-MP}}$= 0.0801. The slope of the line is -0.073. The T_{DCP} is 76.25°C.

Δ $T < T_{DCP}$

∇ $T > T_{DCP}$

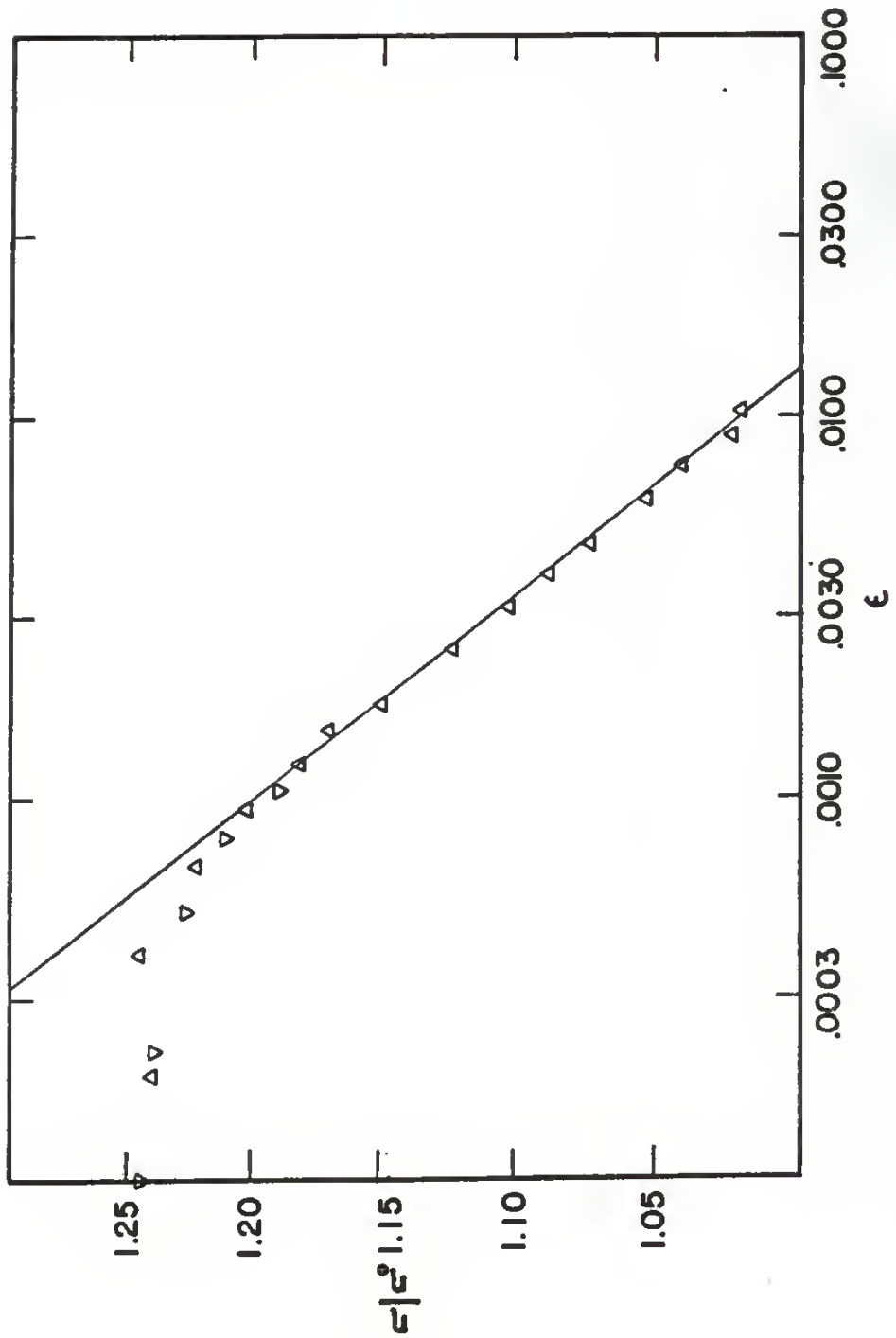
1.25
1.20
1.15
1.10
1.05
$\epsilon^{-1}|\epsilon|^{0.9}$
.0003
.0010
.0030
.0100
.0300
.1000
ϵ

Figure 17. On a log-log scale, η/η_0 is plotted versus ε. For this mixture, X_{H_2O}=0.7987, X_{D_2O}=0.1241, and $X_{3\text{-MP}}$= 0.0773. The slope of the line is -0.068. The T_{DCP} is 76.00°C.

Δ $T < T_{DCP}$

∇ $T > T_{DCP}$

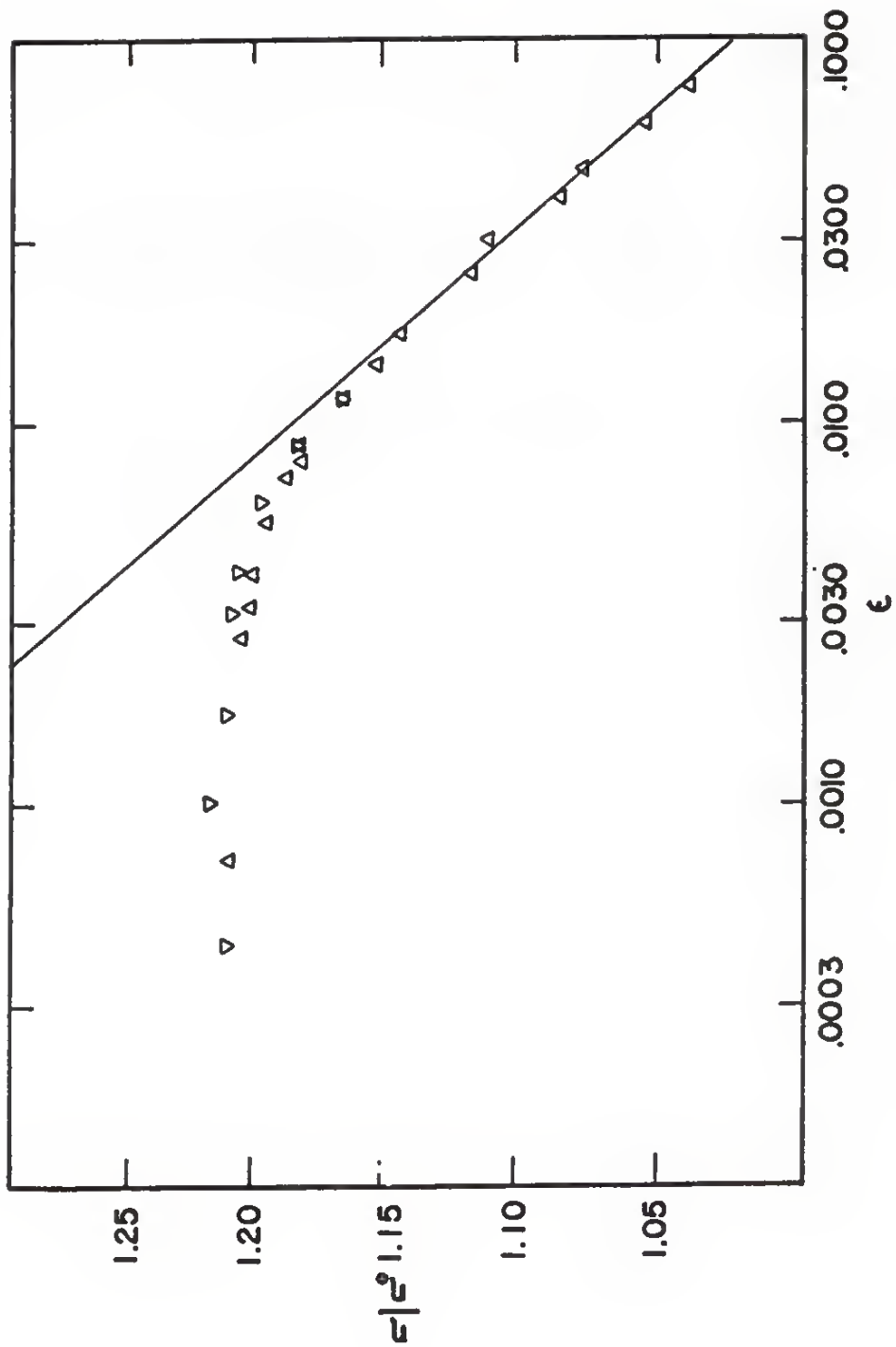
1.25
1.20
1.15
1.10
1.05
$\tau = |\epsilon|^{\beta}$
.0003
.0010
.0030
.0100
.0300
.1000
ϵ

Figure 18. On a log-log scale, η/η_o is plotted versus ε. For this mixture, X_{H_2O}=0.8020, X_{D_2O}=0.1207, and $X_{3\text{-MP}}$= 0.0772. The slope of the line is -0.067. The T_{DCP} is 76.00°C.

Δ $T < T_{DCP}$

∇ $T > T_{DCP}$

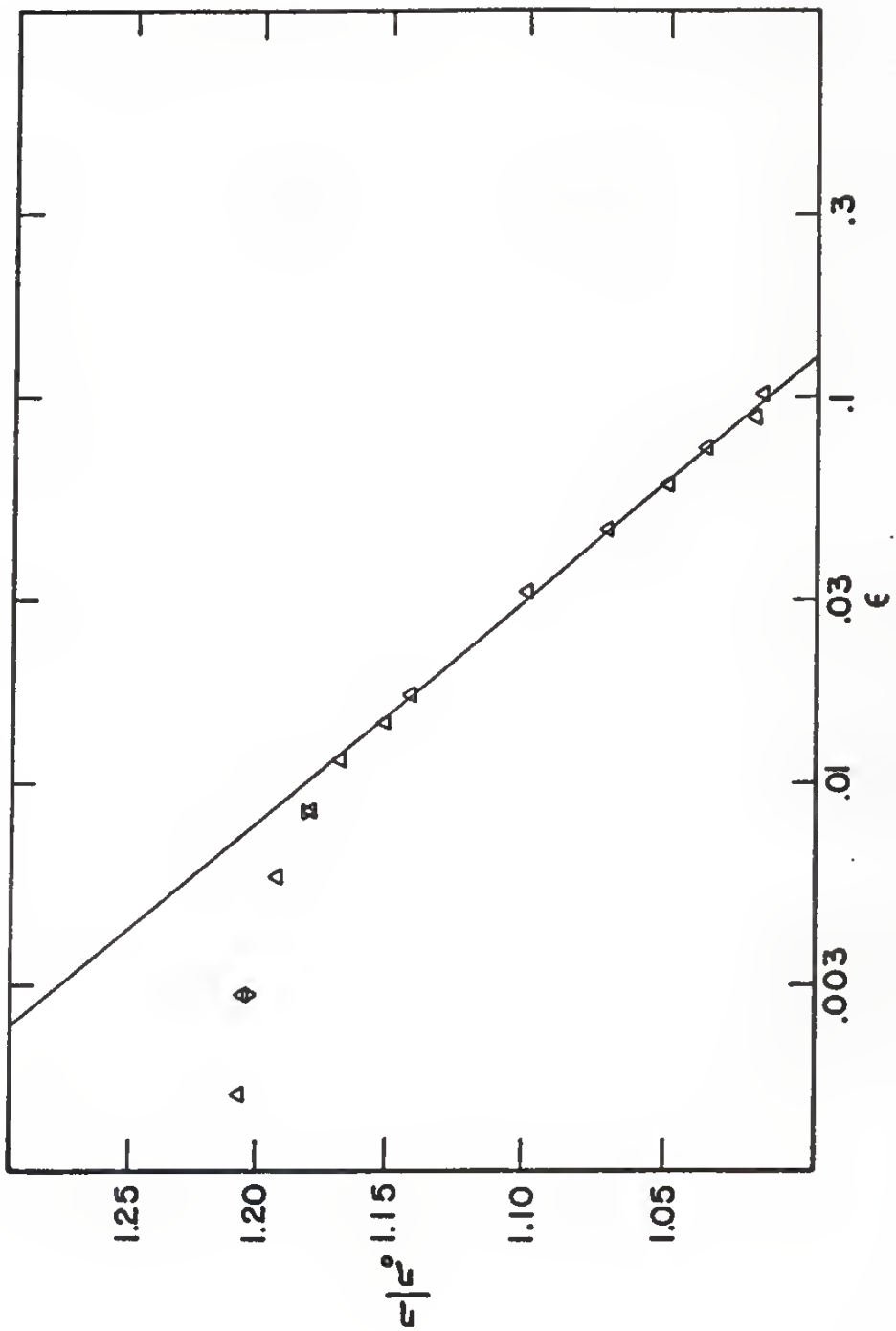
1.25
1.20
1.15
1.10
1.05
$\tau = |\epsilon|^{2\beta}$
.3
.1
.03
.01
.003
ϵ

Figure 19. On a log-log scale, η/η_0 is plotted versus ε. For this mixture, X_{H_2O}=0.8061, X_{D_2O}=0.1165, and $X_{3\text{-MP}}$= 0.0774. The slope of the line is -0.073. The T_{DCP} is 76.45°C.

$\triangle$ $T < T_{DCP}$

∇ $T > T_{DCP}$

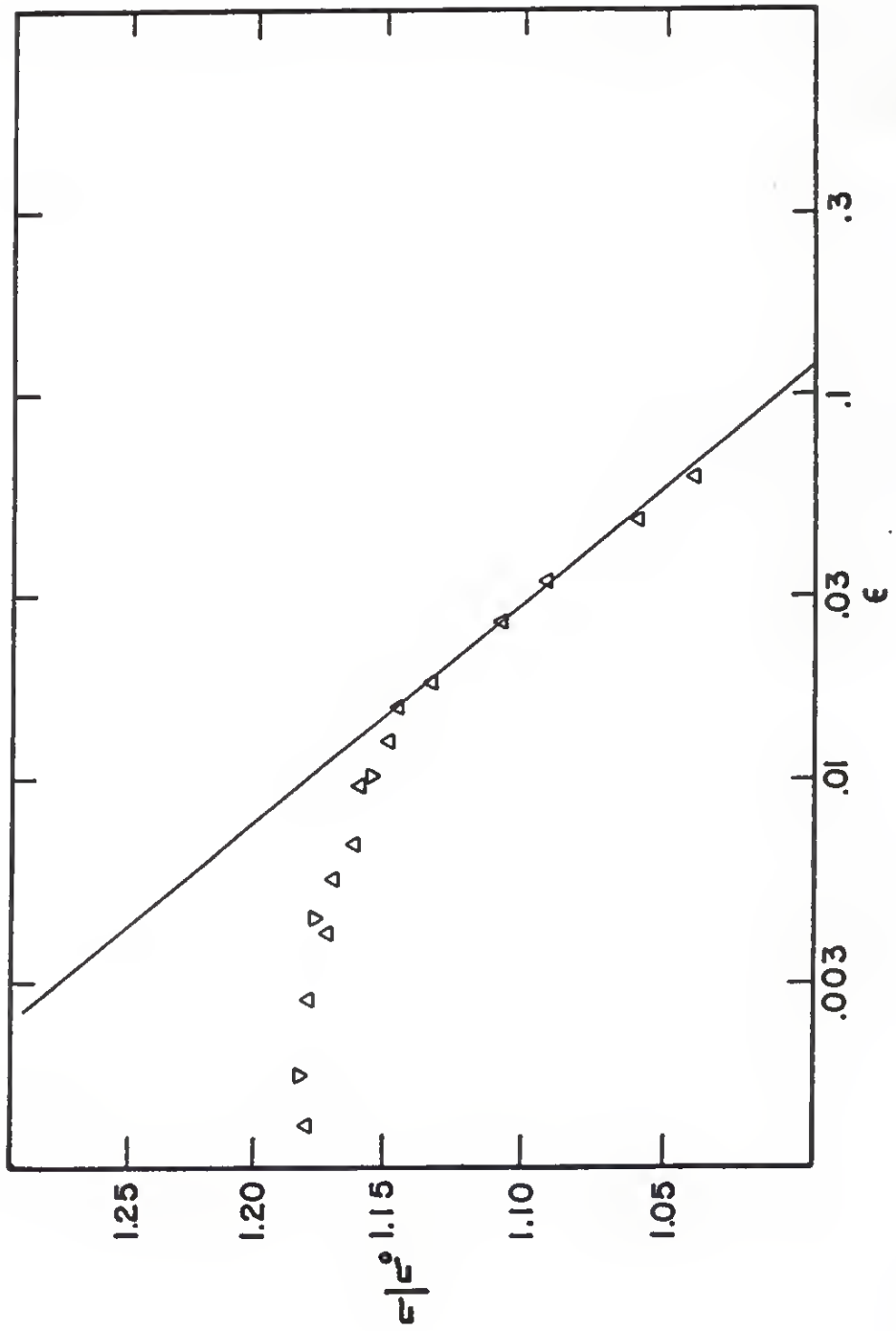
1.25
1.20
1.15
1.10
1.05
$\sigma = |\epsilon|^{\beta}$
.003
.01
.03
.1
.3
ϵ

Figure 20. On a log-log scale, η/η_o is plotted versus ε. For this mixture, X_{H_2O}=0.9238, X_{D_2O}=0.0000, and $X_{3\text{-MP}}$= 0.0762. The slope of the line is -0.07. The T_{DCP} is 76.00°C.

Δ $T < T_{DCP}$

∇ $T > T_{DCP}$

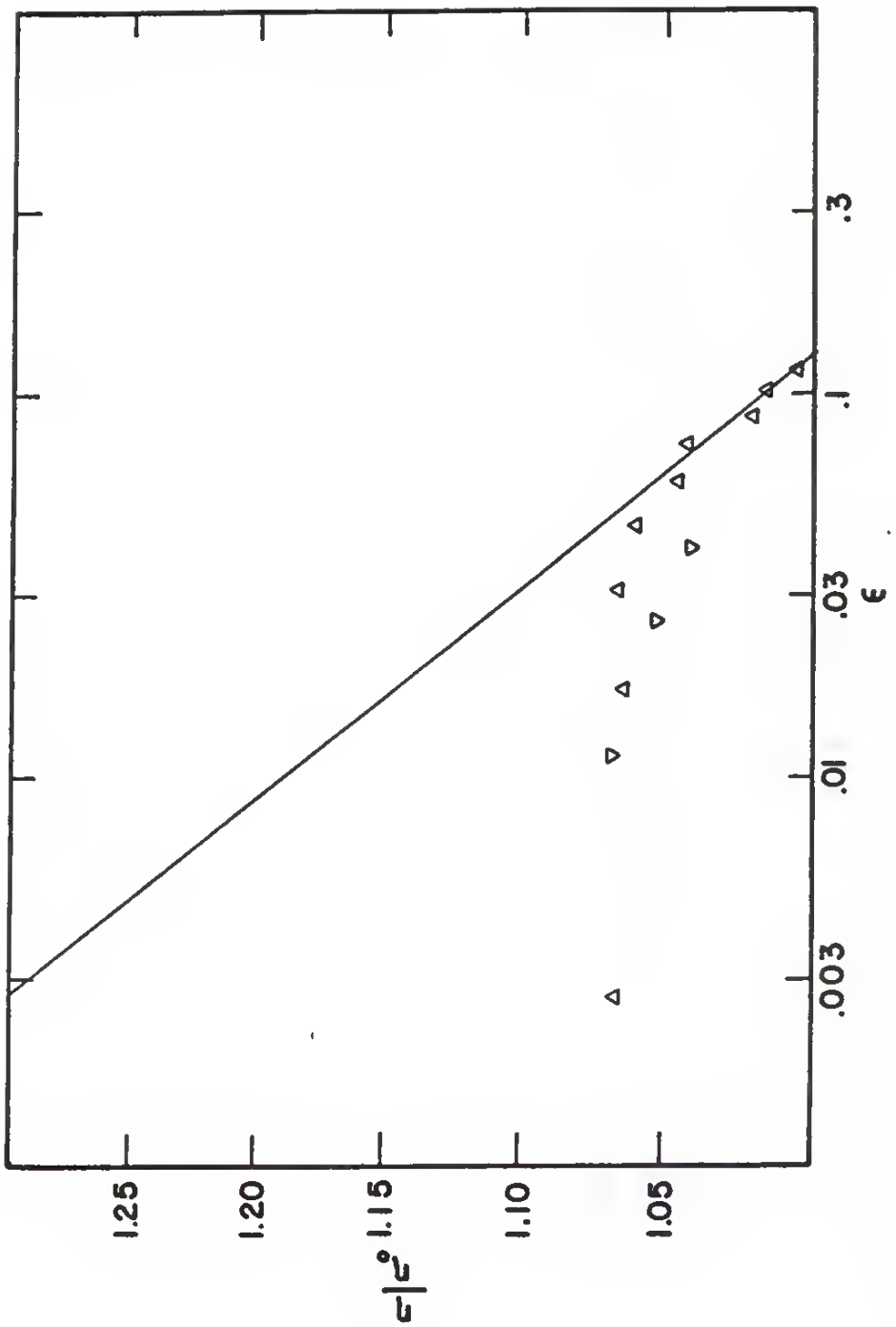
1.25
1.20
1.15
1.10
1.05
τ/τ°
.3
.1
.03
.01
.003
ϵ

Figure 21. Shown is a composite of Figs. 16-20. Open symbols indicate $T < T_{DCP}$. Closed symbols indicate $T > T_{DCP}$.

△	X_{H_2O}=0.7954	X_{D_2O}=0.1245	$X_{3\text{-MP}}$=0.0801
○	X_{H_2O}=0.7987	X_{D_2O}=0.1241	$X_{3\text{-MP}}$=0.0773
□	X_{H_2O}=0.8020	X_{D_2O}=0.1207	$X_{3\text{-MP}}$=0.0772
⬡	X_{H_2O}=0.8061	X_{D_2O}=0.1165	$X_{3\text{-MP}}$=0.0774
◇	X_{H_2O}=0.9238	X_{D_2O}=0.0000	$X_{3\text{-MP}}$=0.0762

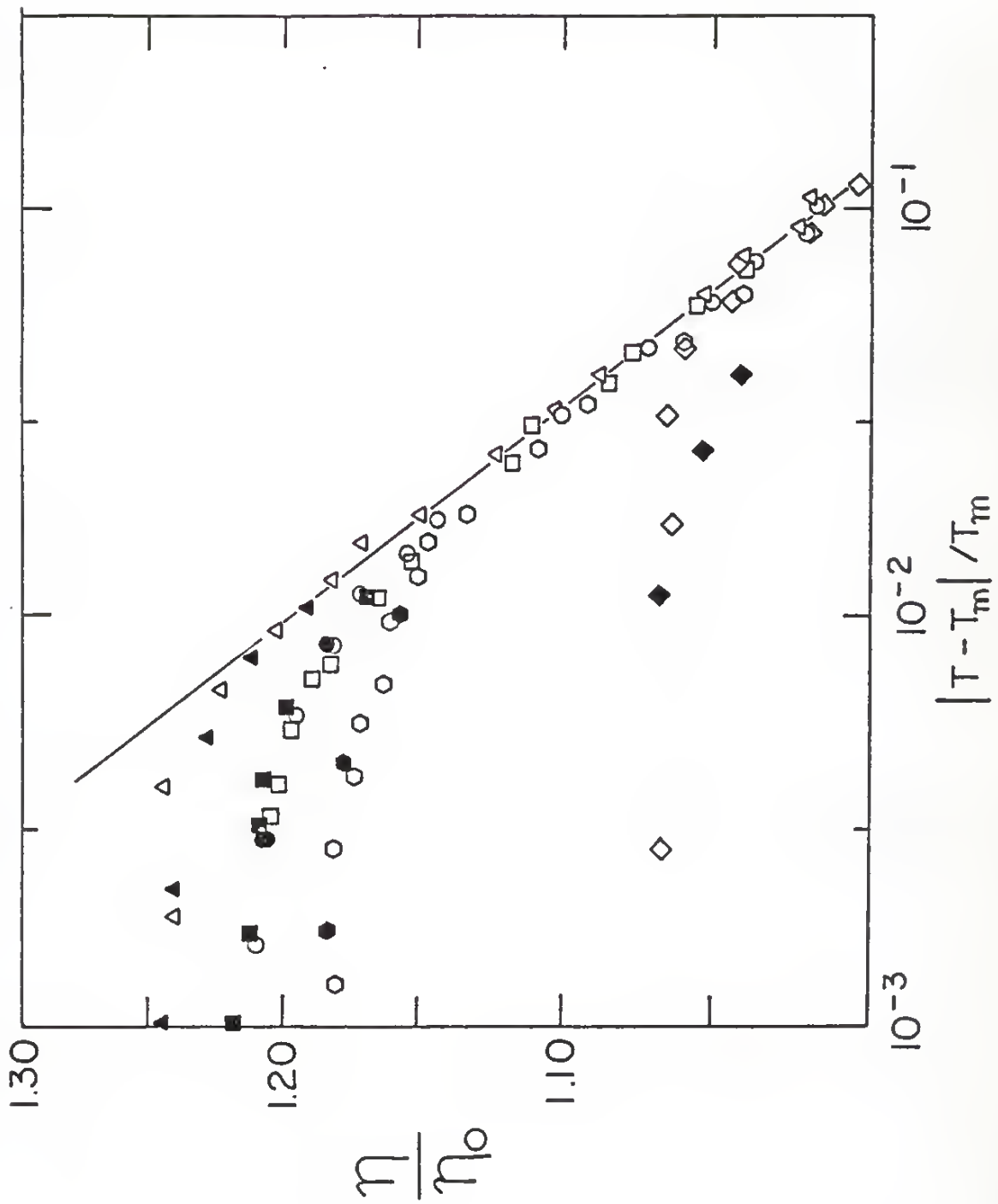
1.30
1.20
1.10
$\frac{\eta}{\eta_0}$
10^{-3}
10^{-2}
10^{-1}
$|T - T_m| / T_m$

Table III. This table lists our results for the shear viscosity critical exponents, ϕ, of the various mixtures. X_{H_2O}, X_{D_2O}, and $X_{3\text{-MP}}$ are the mole-percent concentrations of H_2O, D_2O, and 3-methylpyridine, respectively.

TABLE III

Solution Number	X_{H_2O}	X_{D_2O}	$X_{3\text{-mp}}$	ϕ
1	0.0000	0.9160	0.0840	0.038
2	0.3914	0.5279	0.0807	0.050
3	0.7356	0.1866	0.0778	0.051
4	0.7926	0.1298	0.0776	0.064
5	0.7880	0.1290	0.0830	0.072
6	0.7954	0.1245	0.0801	0.073
7	0.7987	0.1241	0.0773	0.068
8	0.8020	0.1207	0.0772	0.067
9	0.8061	0.1165	0.0774	0.073
10	0.9238	0.0000	0.0762	0.07

At a given value of ε, which increased as the solution concentration receded further from the critical isochore, $\eta(T)/\eta_0(T)$ stopped increasing with decreasing ε and leveled off. Rather than decreasing with increasing distance from the double critical point as for separating solutions, the shear viscosity critical exponent remained roughly constant with an average value of 0.070.

KORTAN ANALYSIS

In the introduction, we discussed an expression developed by Kortan, et al.,[6] to describe the behavior of the correlation length of a binary solution near a double critical point. This expression was

$$\xi = \xi^0[\varepsilon + (T_c/\Delta T)\varepsilon^2]^{-\nu} \tag{3-5}$$

where ξ is the correlation length, ξ^0 is concentration dependent, ΔT is the separation between upper and lower critical temperatures, and ν is the correlation length critical exponent for a single critical point. We may express the shear viscosity as[10]

$$\eta = \eta_0(\xi\Lambda)^{\phi/\nu} \tag{3-6}$$

so that Eq. (3-5) can be modified to

$$\varepsilon^{-1}\Lambda^{1/\nu}(\eta/\eta_0)^{-1/\phi} = (\xi^0)^{-1/\nu}[1 + (T_c/\Delta T)\varepsilon] \tag{3-7}$$

Λ is a microscopic cut-off wave number. It should be independent of temperature and so

$$\varepsilon^{-1}(\eta/\eta_0)^{-1/\phi} \sim (\xi^0)^{-1/\nu} + (\xi^0)^{-1/\nu}(T_c/\Delta T)\varepsilon \quad .$$

If Eq. (3-7) is correct, then a plot of $\varepsilon^{-1}(\eta/\eta_0)^{-1/\phi}$ versus ε will yield

a straight line for each separating solution. The value of ϕ we used in this expression was near the predicted value for a single critical point, 0.040. The slope for a given solution should be equal to $(\xi^o)^{-1/\nu}(T_c/\Delta T)$ and the intercept should be $(\xi^o)^{-1/\nu}$. ν is the correlation length critical exponent and the value used is that predicted for a single critical point, 0.65. According to Johnston,[16] ξ^o increases as the double critical point is approached. So, the intercept should decrease as the double critical point is approached. Whether the slope increases, decreases, or remains the same depends upon how rapidly $T_c/\Delta T$ increases as $(\xi^o)^{-1/\nu}$ decreases.

In Figs. 22 through 27, $\varepsilon^{-1}(\eta/\eta_o)^{-1/\phi}$ is plotted versus ε for the separating solutions. Since it was not known if T_c was the same for a given solution as before, different values for T_c were tried and the results were again judged based on the linearization and the symmetrization of the plots. The agreement with Kortan can only be described as poor. The intercepts do decrease as the double critical point is approached, as expected. However, it was not possible to achieve any real linearization for the three plots furthest from the double critical point, and the other two exhibited poor linearization. Furthermore, in the solution closest to the double critical point, satisfactory symmetrization could not be achieved.

For solutions beyond the double critical point, Kortan found that[6]

$$\xi = A[(T-T_m)^2 + a(y-y_o)]^{-\nu} \qquad (3\text{-}8)$$

or

$$\xi^{-1/\nu} = A^{-1/\nu}(T-T_m)^2 + A^{-1/\nu}a(y-y_o) \qquad (3\text{-}9)$$

where A and a are constants. T_m is the double critical point temperature and y_o is the concentration at the double critical point of the binary solution. Manipulating and substituting for ξ in Eq. (3-9), this expression

Figure 22. On a linear scale, $\varepsilon^{-1}(\eta/\eta_o)^{-25}$ is plotted versus ε. For this mixture, X_{H_2O}=0.0000, X_{D_2O}=0.9160, and $X_{3\text{-MP}}$= 0.0840. The LCST is 37.36°C.

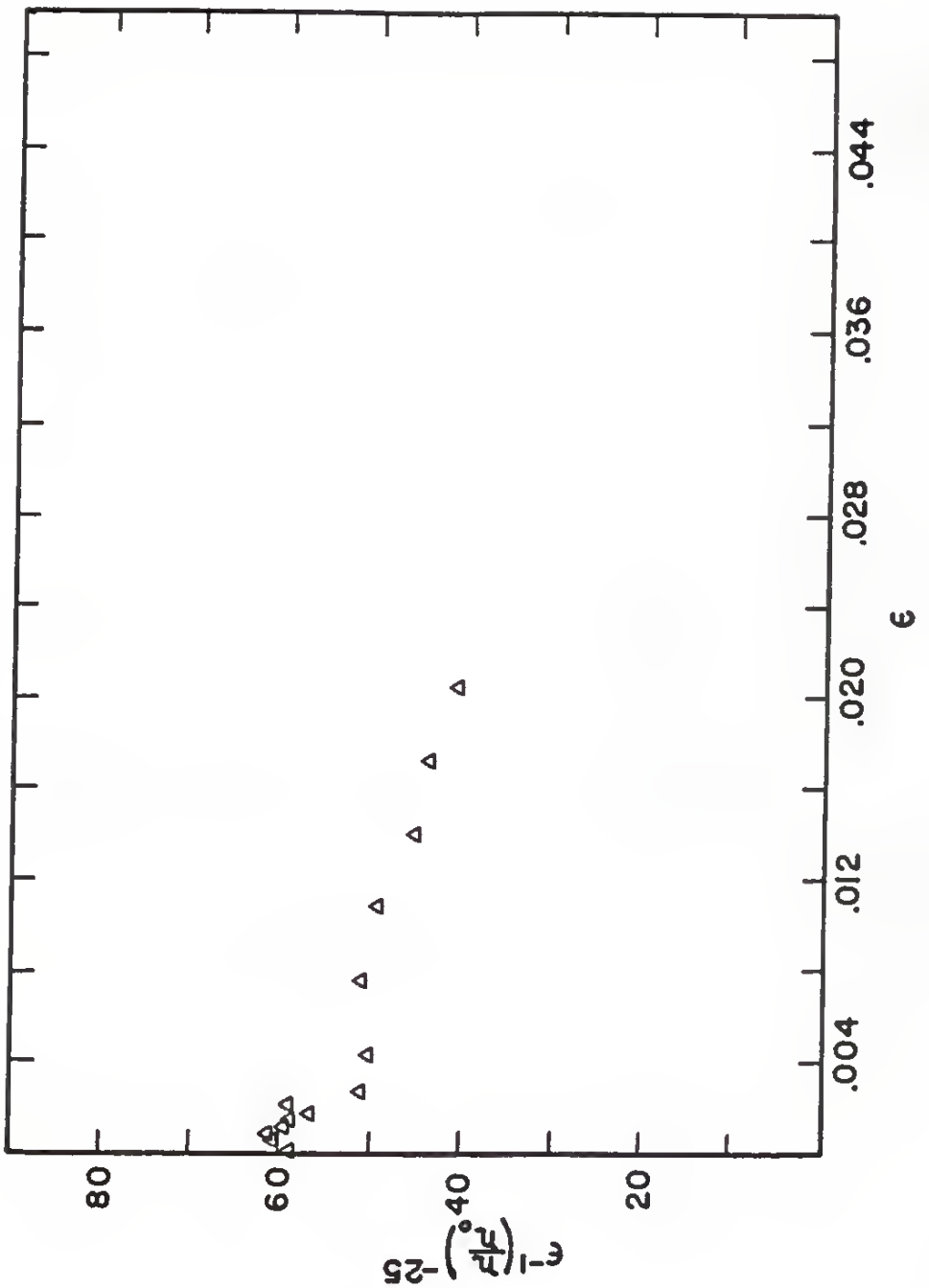
80
60
40
20
.004
.012
.020
.028
.036
.044
ε
ε⁻¹(dP/dε)₁₋₃ -25

Figure 23. On a linear scale, $\varepsilon^{-1}(n/n_0)^{-25}$ is plotted versus ε. For this mixture, X_{H_2O}=0.3914, X_{D_2O}=0.5279, and $X_{3\text{-MP}}$= 0.0807. The LCST is 48.46°C.

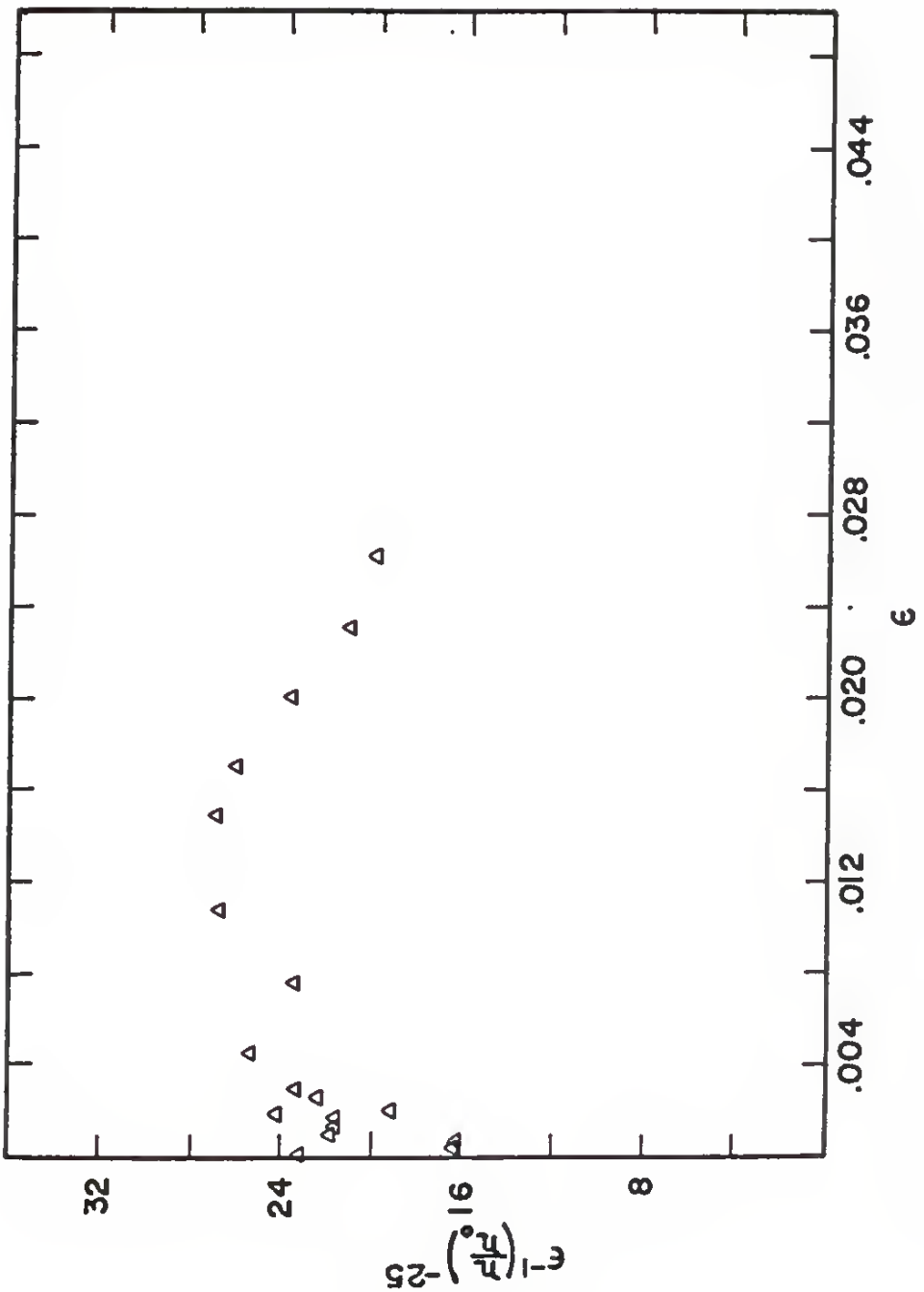
32
24
16
8
.004
.012
.020
.028
.036
.044
ε
$\epsilon^{-1}\left(\frac{\pi r_p}{r_0}\right)^{-25}$

Figure 24. On a linear scale, $\varepsilon^{-1}(n/n_0)^{-25}$ is plotted versus ε. Five different temperature choices for the LCST are shown to demonstrate the sensitivity of the system to our choice of the LCST. For this mixture, X_{H_2O}= 0.7356, X_{D_2O}=0.1866, and $X_{3\text{-MP}}$=0.0778.

□ LCST = 63.80°C

△ LCST = 63.85°C

● LCST = 63.90°C

○ LCST = 63.95°C

▲ LCST = 64.00°C

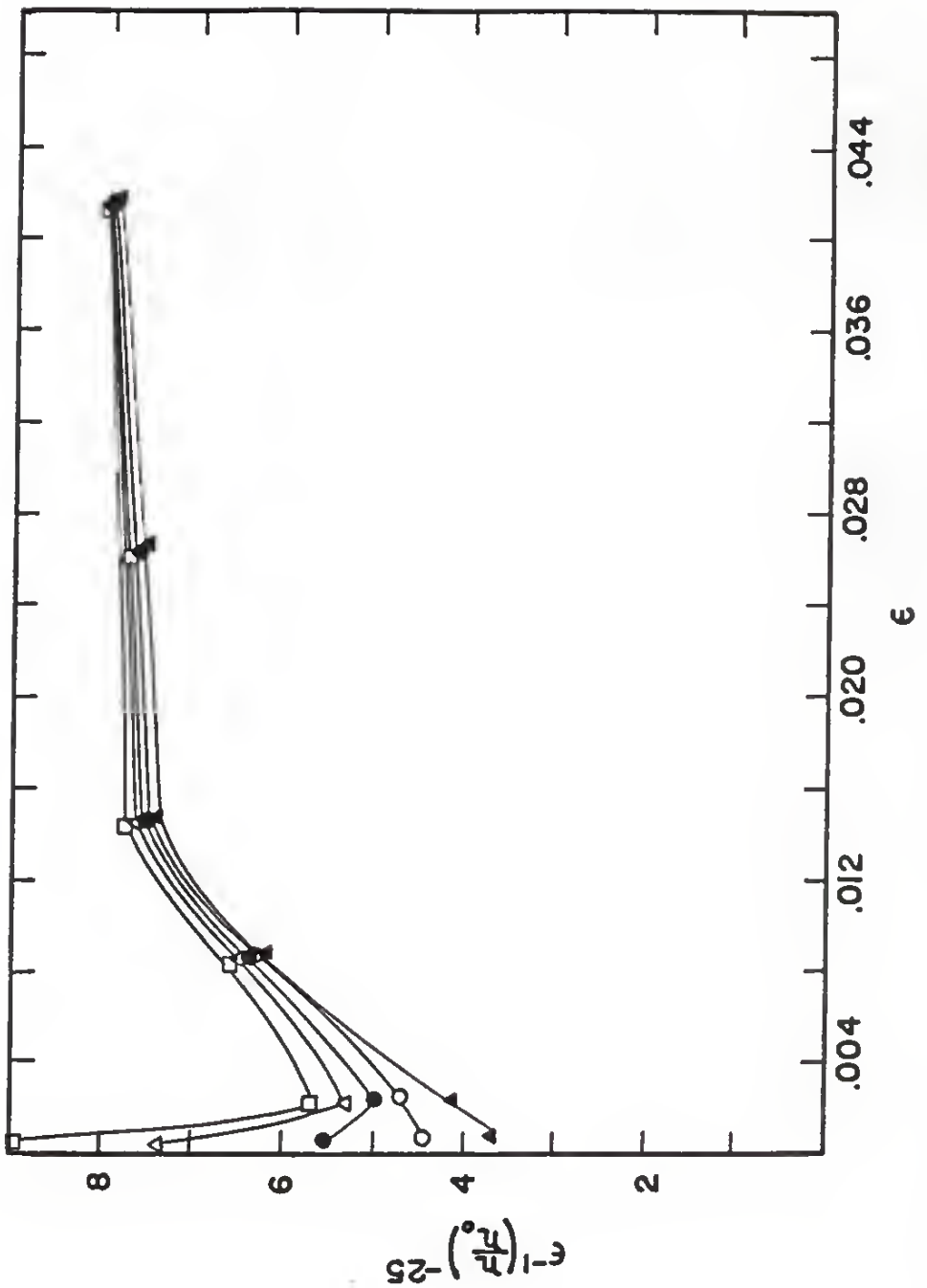
8
6
4
2
.004
.012
.020
.028
.036
.044
ε
$\epsilon^{-1}\left(\frac{\Delta T_c}{T_{c_0}}\right)^{-25}$

Figure 25. On a linear scale, $\varepsilon^{-1}(\eta/\eta_0)^{-25}$ is plotted versus ε. For this mixture, X_{H_2O}=0.7926, X_{D_2O}=0.1298, and $X_{3\text{-MP}}$=0.0776. The LCST is 74.00°C.

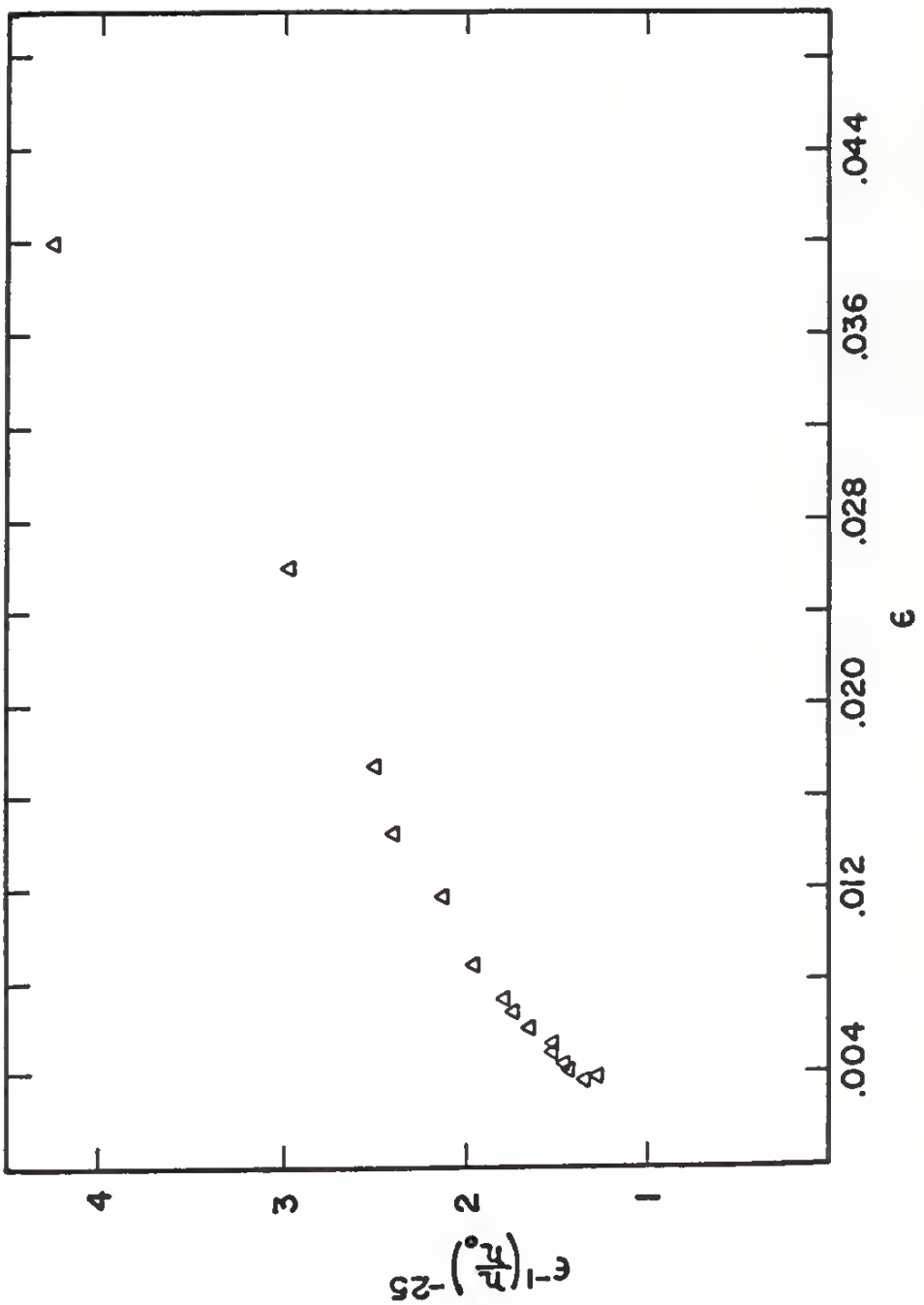
$\epsilon^{-1}\left(\frac{T_c}{T_{c_0}}\right)^{-25}$
1
2
3
4
.004
.012
.020
.028
.036
.044
ϵ

Figure 26. On a linear scale, $\varepsilon^{-1}(\eta/\eta_0)^{-25}$ is plotted versus ε. For this mixture, X_{H_2O}=0.7880, X_{D_2O}=0.1290, and $X_{3\text{-MP}}$=0.0830. The LCST is 75.5°C and the UCST is 77.5°C.

△ T< LCST = 75.5°C

▽ T> UCST = 77.5°C

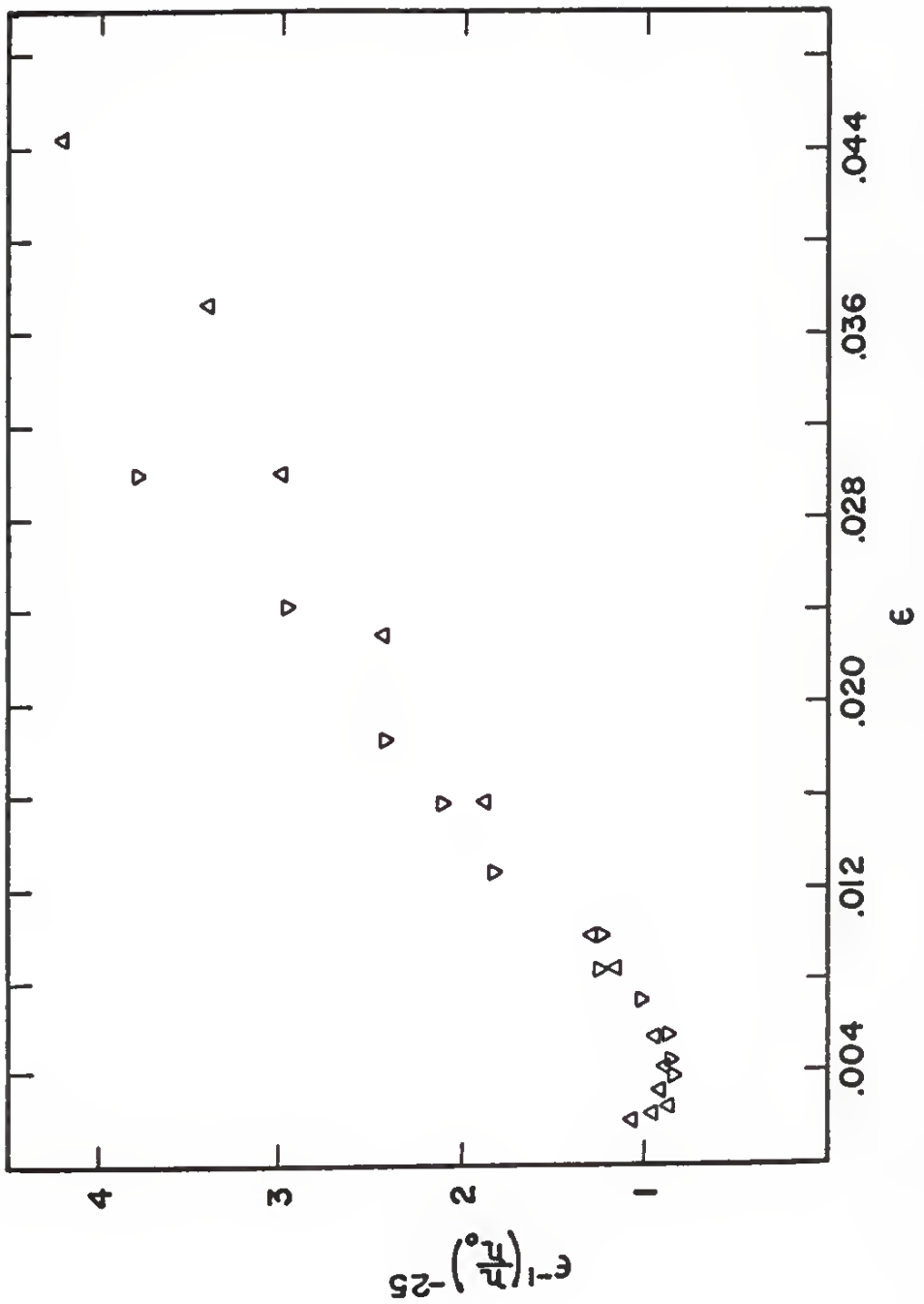
$\epsilon^{-1}\left(\frac{T_c}{T_{c_0}}\right)^{-25}$
4
3
2
1
.004
.012
.020
.028
.036
.044
ϵ

Figure 27. This is a composite figure with $\varepsilon^{-1}(\eta/\eta_o)^{-25}$ plotted versus ε on a linear scale for three of the solutions that phase separated. While the intercepts do decrease as the double critical point is approached (as predicted), it is easy to see that the graphs exhibit poor linearity.

X_{H_2O}=0.7356 X_{D_2O}=0.1866 $X_{3\text{-MP}}$=0.0778

X_{H_2O}=0.7926 X_{D_2O}=0.1298 $X_{3\text{-MP}}$=0.0776

(T<LCST) X_{H_2O}=0.7880 X_{D_2O}=0.1290

(T>UCST) $X_{3\text{-MP}}$=0.0830

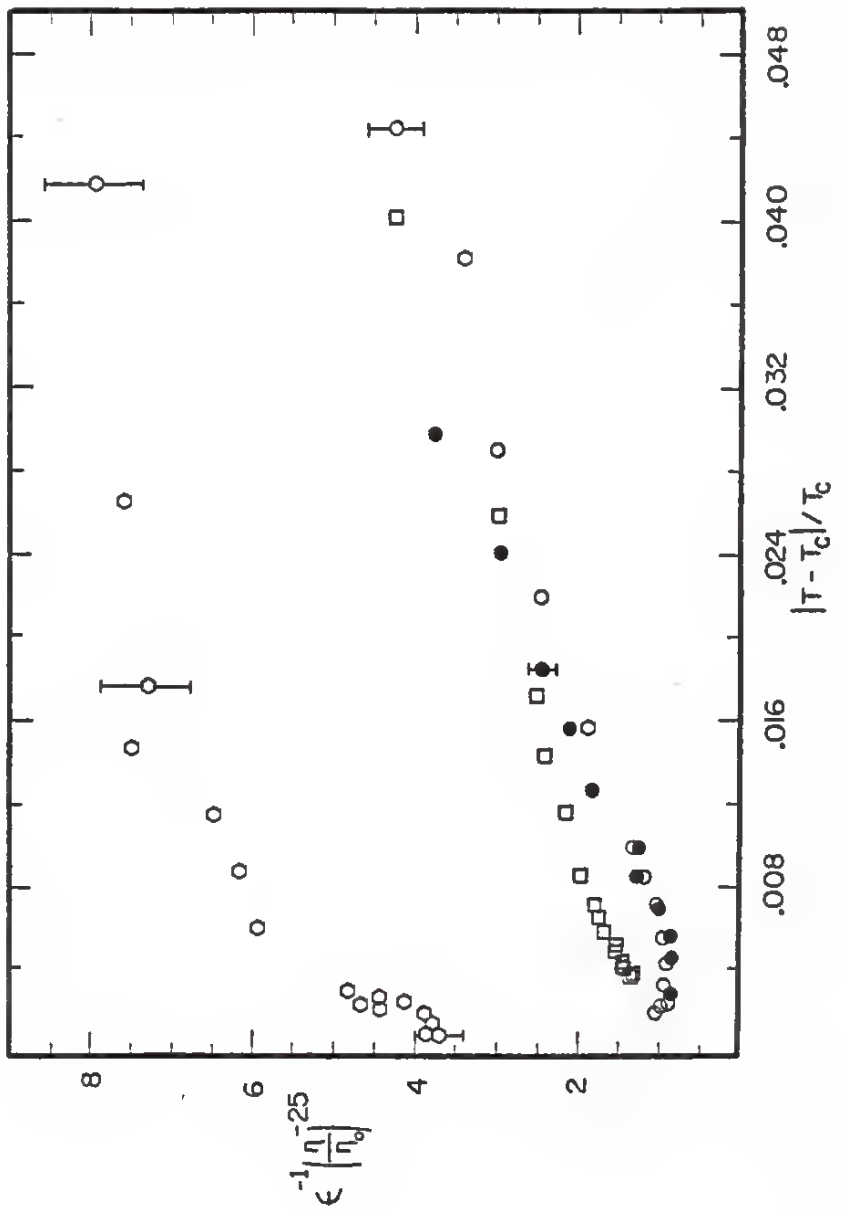
8
6
4
2
$\epsilon^{-1}\left|\frac{n}{n_o}\right|^{-25}$
.008
.016
.024
.032
.040
.048
$|T - T_c|/T_c$

becomes

$$\Lambda^{1/\nu}(\eta/\eta_o)^{-1/\phi} = A^{-1/\nu}\,(T-T_m)^2 + A^{-1/\nu}\,a(y-y_o) \qquad (3\text{-}10)$$

If we again assume Λ is independent of temperature, then a plot of $(\eta/\eta_o)^{-1/\phi}$ versus $(T-T_m)^2$ should yield a straight line. The slopes for these solutions will definitely not change with concentration. However, the intercept again will get smaller as the critical concentration is approached, in fact going to zero as y approaches y_o.

In Figs. 28 through 32, $(\eta/\eta_o)^{-1/\phi}$ is plotted versus $(T-T_m)^2$ for four of the five non-separating systems. T_m is 76°C for all four solutions. The H_2O/3-methylpyridine solution has been excluded. All four curves are very linear and the symmetrization is also quite good.

A least squares fit was also performed on the data of these four mixtures for $|T-T_m|^2$ less than 200 $(^oC)^2$. The resultant slopes for the first three were all within 2.5% of the average. The slope of the fourth was somewhat higher than the other three. In addition, the value of the intercept divided by the slope, which is equal to $a(y-y_o)$, scales properly, decreasing as the double critical point concentration is approached. The agreement with Kortan is quite good for these mixtures.

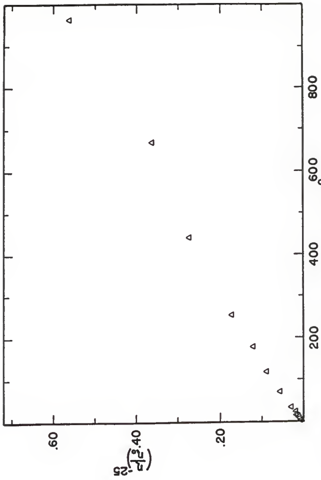
.60
.40
.20
200
400
600
800
|T-76°C|²

Figure 29. On a linear scale, $(\eta/\eta_0)^{-25}$ is plotted versus $|T-76^{o}C|^{2}$. For this mixture, $X_{H_2O}=0.7987$, $X_{D_2O}=0.1241$, and $X_{3\text{-MP}}=0.0773$.

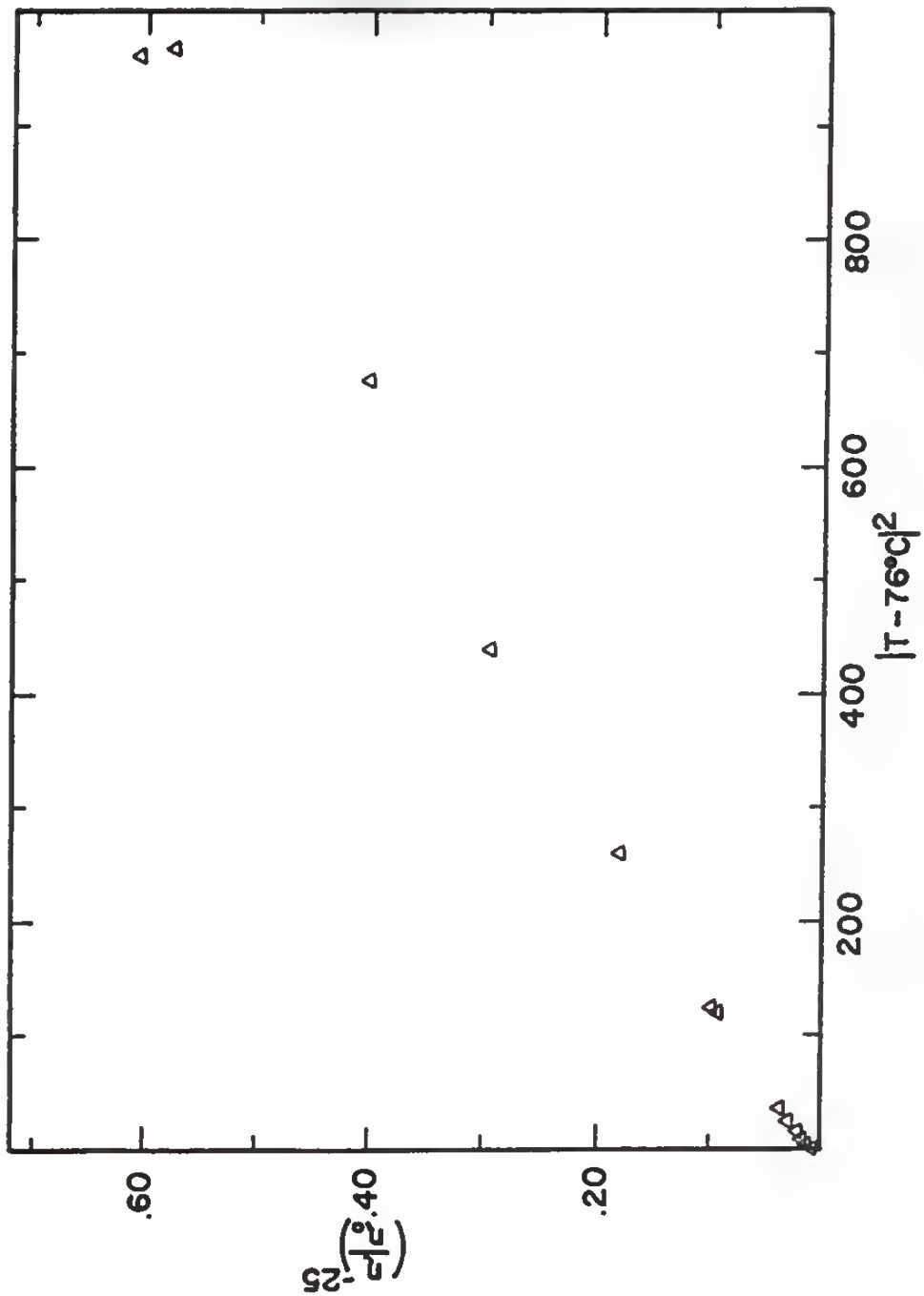
.60
.40
.20
200
400
600
800
$|T-76°C|^2$
$\left(\frac{\partial^2 P}{\partial T^2}\right)^{-2.25}$

Figure 30. On a linear scale, $(\eta/\eta_0)^{-25}$ is plotted versus $|T-76^{\circ}C|^2$. For this mixture, $X_{H_2O}=0.0820$, $X_{D_2O}=0.1207$, and $X_{3\text{-MP}}=0.0772$.

△ $T<76^{\circ}C$

▽ $T>76^{\circ}C$

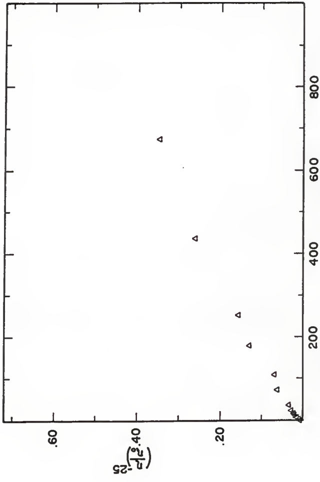

.60
.40
.20
200
400
600
800
|T-76°C|²

Figure 31. On a linear scale, $(\eta/\eta_o)^{-25}$ is plotted versus $|T-76^oC|^2$. For this mixture, $X_{H_2O}=0.8061$, $X_{D_2O}=0.1165$, and $X_{3\text{-MP}}=0.0774$.

△ $T<76^oC$

▽ $T>76^oC$

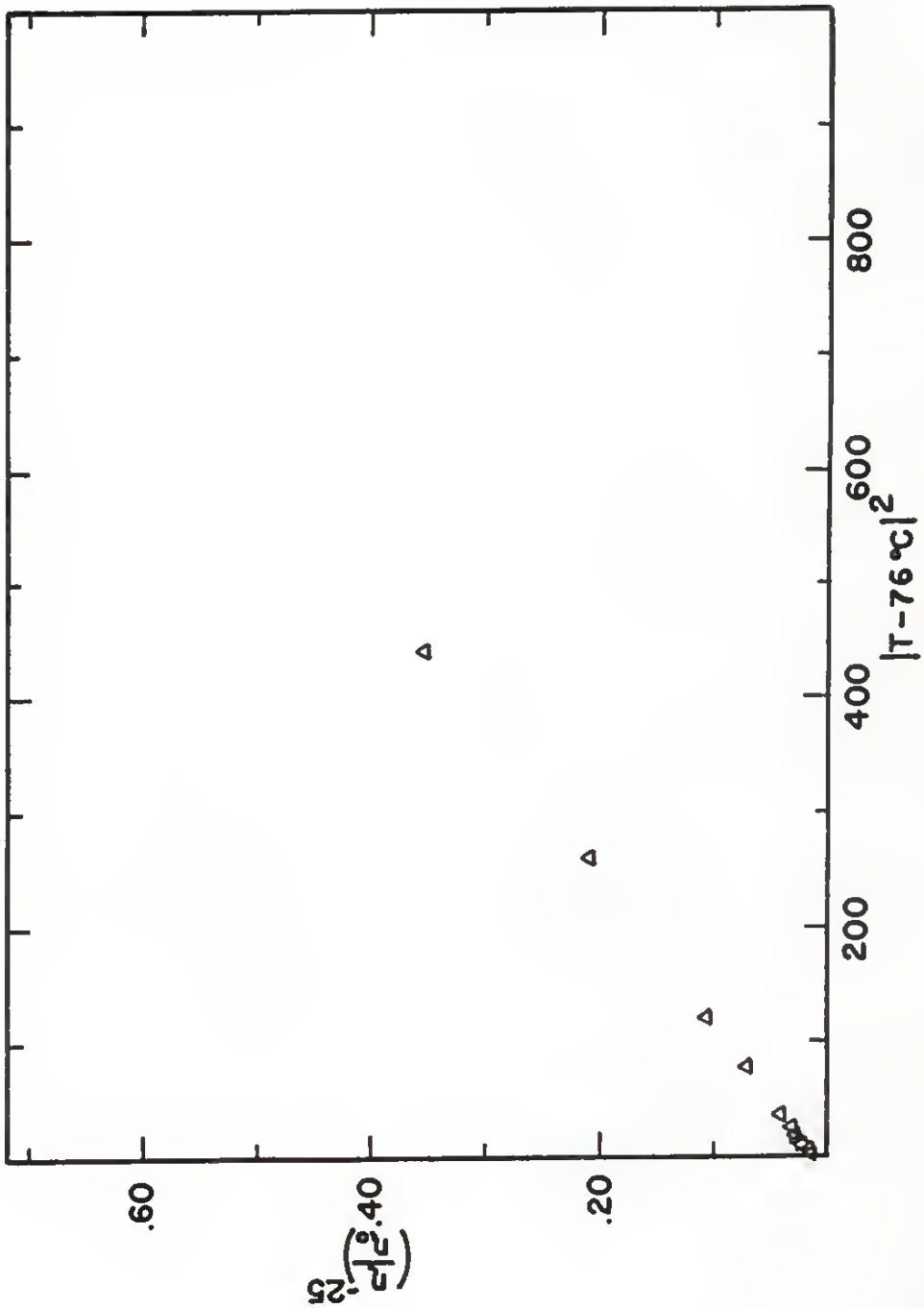
.60
.20
$\left(\frac{dP}{dT}\right)^{.25}$
200
400
600
800
$|T-76\,^{\circ}C|^2$

Figure 32. This is a composite figure with $(\eta/\eta_0)^{-25}$ plotted versus $|T-76^oC|^2$ on a linear scale for the four solutions shown in Figs. 28-31. The ordinate axis values have been shifted for three solutions as shown below. Open symbols are for $T<76^oC$ and closed symbols are for $T>76^oC$.

△ $X_{H_2O}=0.7954$ $X_{D_2O}=0.1245$ $X_{3\text{-MP}}=0.0801$
no shift

○ $X_{H_2O}=0.7987$ $X_{D_2O}=0.1241$ $X_{3\text{-MP}}=0.0773$
shifted by +0.04

□ $X_{H_2O}=0.8020$ $X_{D_2O}=0.1207$ $X_{3\text{-MP}}=0.0772$
shifted by +0.08

⬡ $X_{H_2O}=0.8061$ $X_{D_2O}=0.1165$ $X_{3\text{-MP}}=0.0774$
shifted by +0.12

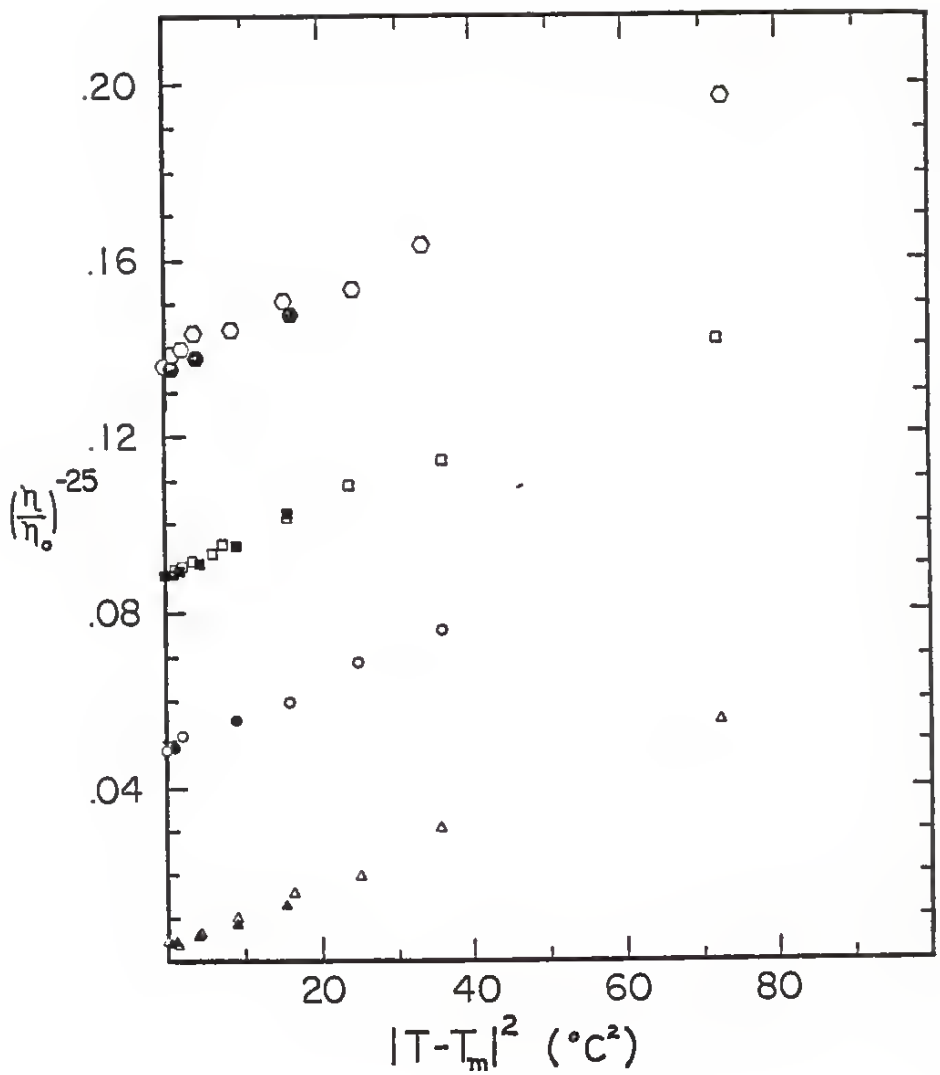
.20
.16
.12
.08
.04
$\left(\frac{\eta}{\eta_o}\right)^{-25}$
20
40
60
80
$|T-T_m|^2$ (°C²)

Chapter IV

CONCLUSION

The behavior of the shear viscosity of a ternary liquid was studied both far from and in the immediate vicinity of a double critical point. We believed that this system was more properly viewed as quasi-binary, rather than ternary, because of its composition. As such, it was felt that the behavior of the shear viscosity critical exponent would mirror the behavior in a true binary system. In particular, we were interested in finding evidence to support or reject the prediction proposed by others[1-4] that the exponent would double as the double critical point was approached.

The value of the critical exponent was definitely seen to increase as we got close to the double critical point. It nearly doubled, increasing from 0.038 for D_2O/3-methylpyridine to 0.072 for the solution of H_2O/D_2O/3-methylpyridine closest to the critical concentration. Beyond the double critical point, the critical exponent was seen to remain roughly constant at approximately 0.070 for data far from T_{DCP}. We see this as strong evidence in favor of critical exponent doubling at a double critical point for a binary system.

It might be argued that this is not a quasi-binary system, as proposed, but is a true ternary system. When examining the critical exponents of a ternary system, we see that they must be renormalized from the binary system values. It has been shown that both the correlation length critical exponent,[17] ν, and the coexistence-curve critical exponent,[18,19] β, must be renormalized by $(1-\alpha)^{-1}$, where α is the heat capacity critical exponent and

is approximately equal to 0.12. If the shear viscosity critical exponent can be similarly renormalized, then it is approximately equal to $(0.04)(0.88)^{-1}$ or 0.046. S. P. Lee has experimentally determined the value of this exponent[20] to be equal to about 0.053 for a water-ethanol-chloroform system. Looking at Table III, we see two solutions, #2 and #3, with experimentally measured values equal to 0.050 and 0.051, respectively. When closest to the double critical point with solution #5, the critical exponent has increased to 0.072. This is an increase of about 57% over the theoretical value and 36% over Lee's experimental value.

Given the behavior of this system, however, the hypothesis that this is a quasi-binary system seems reasonable. As the coexistence loop was gradually shrunk, bringing the upper and lower critical solution temperatures closer together, the shear viscosity critical exponent gradually increased from 0.038 to 0.072. The final value is almost double the exponent value when far from the double critical point. It remained roughly constant with an average value of 0.070 as we progressed beyond the miscibility dome far from the double critical point.

In addition, an attempt was made to compare our data with two expressions developed by Kortan et al.[6] to describe phenomenologically the behavior of the correlation length in a reentrant liquid crystal near a double critical point. These expressions predict that the shear viscosity critical exponent will gradually double as the miscibility loop shrinks sufficiently and will remain at the doubled value after the loop disappears completely. This is in qualitative agreement with what we saw. For the non-separating systems, the data agreed quite well with the appropriate expression. For our separating systems, the quantitative agreement was poor unless we were close to the double critical point. It is possible that the viscosity anomaly was

weak enough that the statistical scatter in the data was too large to allow us to compare this data with Kortan. A standard deviation of 0.3% in $n(T)/n_0(T)$ leads to a standard deviation of about 8% in $[n(T)/n_0(T)]^{-25}$. If so, it would be necessary to approach T_c much more closely and with more precision in order to properly test Kortan's expression for a separating system than was possible in our experiment.

TABLE IV

Solution #1

X_{H_2O}=0.0000 X_{D_2O}=0.09160 $X_{3\text{-mp}}$=0.0840

Temp (^oC)	10^3K (cp-cm^3/g-s)	Density (g/cm^3)	Flowtime (s)	η (cp)
5.00	8.341	1.081	575.5	5.189
10.00	8.318	1.077	462.7	4.145
15.00	8.296	1.074	381.8	3.402
20.00	8.273	1.070	322.9	2.858
25.00	8.251	1.066	278.0	2.445
27.00	8.242	1.065	265.3	2.329
28.00	8.237	1.064	257.0	2.252
29.00	8.233	1.064	250.6	2.195
30.00	8.228	1.063	244.7	2.140
31.00	8.224	1.062	239.4	2.091
32.00	8.219	1.061	234.2	2.042
33.00	8.215	1.061	229.7	2.002
34.00	8.210	1.060	225.7	1.964
35.00	8.206	1.059	222.9	1.937
36.00	8.201	1.059	222.6	1.933
36.50	8.199	1.058	223.9	1.942
36.70	8.198	1.058	223.9	1.942
36.80	8.197	1.058	225.2	1.953
36.90	8.197	1.058	226.1	1.961
37.00	8.197	1.058	227.5	1.973
37.10	8.196	1.058	229.7	1.992
37.20	8.196	1.058	233.5	2.025
37.30	8.195	1.058	242.1	2.099

TABLE V

Solution #2

X_{H_2O}=0.3914 X_{D_2O}=0.5279 $X_{3\text{-mp}}$=0.0807

Temp (^oC)	10^3K (cp-cm^3/g-s)	Density (g/cm^3)	Flowtime (s)	η (cp)
10.00	9.820	1.043	358.1	3.668
15.00	9.799	1.040	295.6	3.021
20.00	9.777	1.037	249.8	2.533
25.00	9.756	1.034	215.7	2.177
30.00	9.734	1.031	191.4	1.921
35.00	9.713	1.028	167.7	1.679
40.00	9.691	1.025	151.6	1.507
41.00	9.687	1.025	148.8	1.476
42.00	9.682	1.024	145.6	1.444
43.00	9.678	1.023	142.7	1.414
44.00	9.674	1.023	140.7	1.392
45.00	9.670	1.022	139.0	1.374
46.00	9.665	1.022	138.7	1.369
47.00	9.661	1.021	138.1	1.363
47.50	9.659	1.021	139.4	1.375
47.60	9.658	1.020	140.1	1.381
47.80	9.657	1.020	141.8	1.398
47.85	9.657	1.020	140.8	1.388
47.90	9.657	1.020	141.8	1.398
48.00	9.657	1.020	142.7	1.406
48.10	9.656	1.020	144.4	1.419
48.20	9.656	1.020	146.9	1.448
48.30	9.655	1.020	149.5	1.473
48.40	9.655	1.020	152.9	1.507

TABLE VI

Solution #3

X_{H_2O}=0.7356 X_{D_2O}=0.1866 $X_{3\text{-mp}}$=0.0778

Temp (^oC)	10^3K (cp-cm^3/g-s)	Density (g/cm^3)	Flowtime (s)	η (cp)
30.00	8.228	1.006	211.1	1.747
35.05	8.205	1.002	186.8	1.536
39.95	8.183	0.9992	168.1	1.374
45.00	8.161	0.9958	152.1	1.236
49.90	8.138	0.9926	139.4	1.126
55.00	8.114	0.9892	128.9	1.035
58.00	8.100	0.9872	124.1	0.9923
59.00	8.095	0.9865	122.7	0.9798
60.10	8.090	0.9858	122.0	0.9730
61.00	8.086	0.9852	121.7	0.9695
61.95	8.081	0.9845	121.7	0.9682
63.00	8.076	0.9838	124.0	0.9852
63.10	8.076	0.9838	124.8	0.9915
63.15	8.076	0.9837	125.2	0.9946
63.20	8.075	0.9837	124.9	0.9922
63.30	8.075	0.9836	125.5	0.9968
63.40	8.074	0.9836	126.8	1.007
63.50	8.074	0.9835	127.8	1.014
63.65	8.073	0.9834	129.2	1.025
63.70	8.073	0.9834	130.0	1.032

TABLE VII

Solution #4

X_{H_2O}=0.7926 X_{D_2O}=0.1298 $X_{3\text{-mp}}$=0.0776

Temp (°C)	10^3K (cp-cm^3/g-s)	Density (g/cm^3)	Flowtime (s)	η (cp)
25.00	8.251	1.006	237.3	1.970
30.00	8.228	1.002	209.3	1.726
34.90	8.206	0.9987	184.9	1.515
40.00	8.183	0.9952	165.7	1.349
45.00	8.161	0.9918	149.0	1.206
50.00	8.138	0.9883	136.3	1.096
55.00	8.114	0.9849	125.4	1.002
60.00	8.091	0.9814	117.1	0.9298
65.00	8.067	0.9780	110.9	0.8749
68.00	8.053	0.9759	108.2	0.8503
69.00	8.048	0.9752	107.4	0.8429
69.95	8.043	0.9745	107.1	0.8395
71.00	8.038	0.9738	107.2	0.8391
71.50	8.036	0.9735	107.5	0.8409
71.70	8.035	0.9733	107.6	0.8415
71.95	8.034	0.9732	107.9	0.8436
72.18	8.033	0.9730	108.4	0.8472
72.30	8.032	0.9729	108.4	0.8471
72.48	8.031	0.9728	108.8	0.8500
72.58	8.031	0.9727	109.0	0.8515
72.62	8.031	0.9727	109.1	0.8522
72.68	8.030	0.9727	109.6	0.8560
72.71	8.030	0.9726	109.5	0.8552

TABLE VIII

Solution #5

X_{H_2O}=0.7880 X_{D_2O}=0.1290 $X_{3\text{-mp}}$=0.0830

Temp (^oC)	10^3K (cp-cm^3/g-s)	Density (g/cm^3)	Flowtime (s)	η (cp)
19.8	8.274	1.015	285.2	2.395
25.05	8.250	1.011	243.3	2.029
30.05	8.228	1.007	212.9	1.764
35.00	8.206	1.003	189.6	1.561
40.00	8.183	0.9990	169.5	1.386
44.98	8.161	0.9950	152.9	1.242
50.00	8.138	0.9910	139.3	1.123
55.00	8.114	0.9870	128.5	1.029
60.00	8.091	0.9830	119.4	0.9496
62.50	8.079	0.9810	116.2	0.9209
65.00	8.067	0.9790	113.0	0.8924
67.50	8.055	0.9770	110.5	0.8696
70.00	8.043	0.9750	109.2	0.8563
71.00	8.038	0.9742	109.2	0.8549
72.00	8.034	0.9734	109.4	0.8552
73.00	8.029	0.9726	110.4	0.8625
73.55	8.026	0.9722	110.6	0.8628
74.00	8.024	0.9718	111.3	0.8681
74.35	8.022	0.9715	111.8	0.8717
74.60	8.021	0.9713	112.7	0.8778
74.70	8.021	0.9712	112.6	0.8770
74.80	8.020	0.9712	112.6	0.8769
78.85	8.001	0.9769	104.6	0.8101
79.10	8.000	0.9677	103.4	0.8007
79.50	7.998	0.9674	101.9	0.7881
80.00	7.996	0.9670	99.52	0.7693
80.50	7.993	0.9666	97.41	0.7528
81.00	7.991	0.9662	96.07	0.7418
82.00	7.986	0.9654	92.43	0.7123
83.00	7.981	0.9646	89.96	0.6928
84.00	7.977	0.9638	87.68	0.6742
86.00	7.967	0.9622	83.76	0.6420
88.00	7.958	0.9606	80.21	0.6134

TABLE IX

Solution #6

X_{H_2O}=0.7954 X_{O_2O}=0.1245 $X_{3\text{-mp}}$=0.0801

Temp (°C)	10^3K (cp-cm^3/g-s)	Density (g/cm^3)	Flowtime (s)	η (cp)
22.70	8.261	1.007	256.9	2.137
30.10	8.228	1.002	210.1	1.732
34.85	8.206	0.9985	186.9	1.531
40.15	8.182	0.9948	167.3	1.362
44.95	8.161	0.9916	150.9	1.221
50.10	8.138	0.9880	138.1	1.110
54.95	8.114	0.9847	127.0	1.015
60.00	8.091	0.9813	118.0	0.9368
62.55	8.078	0.9795	114.4	0.9052
65.05	8.067	0.9778	111.1	0.8763
67.50	8.055	0.9761	108.8	0.8554
70.05	8.043	0.9744	106.9	0.8377
71.00	8.038	0.9737	107.2	0.8391
71.95	8.034	0.9731	106.6	0.8333
73.00	8.029	0.9723	106.8	0.8338
73.95	8.024	0.9717	107.1	0.8351
74.90	8.020	0.9710	107.5	0.8372
75.60	8.016	0.9706	105.9	0.8239
76.00	8.015	0.9703	105.9	0.8235
76.60	8.012	0.9699	105.9	0.8229
77.00	8.010	0.9696	103.7	0.8054
78.00	8.005	0.9689	101.2	0.7849
79.00	8.000	0.9682	98.37	0.7620
79.95	7.996	0.9676	95.44	0.7384

TABLE X

Solution #7

X_{H_2O}=0.7987 X_{D_2O}=0.1241 $X_{3\text{-mp}}$=0.0773

Temp (^oC)	10^3K (cp-cm^3/g-s)	Density (g/cm^3)	Flowtime (s)	η (cp)
5.00	8.341	1.019	467.0	3.969
10.00	8.318	1.016	386.3	3.264
15.00	8.296	1.012	324.0	2.721
20.00	8.273	1.009	274.0	2.287
25.00	8.251	1.006	237.4	1.971
30.00	8.228	1.002	209.3	1.726
34.90	8.206	0.9991	185.0	1.517
40.00	8.183	0.9957	165.7	1.350
44.90	8.161	0.9924	149.4	1.210
45.00	8.161	0.9923	148.7	1.204
50.00	8.138	0.9890	136.2	1.096
55.00	8.114	0.9857	125.1	1.001
59.90	8.091	0.9824	116.6	0.9268
64.90	8.067	0.9791	109.6	0.8657
65.00	8.067	0.9790	109.7	0.8664
70.00	8.043	0.9757	105.1	0.8248
71.00	8.038	0.9750	104.4	0.8182
72.00	8.034	0.9743	104.3	0.8164
73.00	8.029	0.9737	103.8	0.8115
74.00	8.024	0.9730	103.3	0.8065
75.00	8.019	0.9723	102.7	0.8007
75.45	8.017	0.9720	102.3	0.7972
76.00	8.015	0.9717	101.6	0.7913
77.00	8.010	0.9710	99.54	0.7742
79.00	8.000	0.9697	94.90	0.7362

TABLE XI

Solution #8

X_{H_2O}=0.8020 X_{D_2O}=0.1207 $X_{3\text{-mp}}$=0.0772

Temp (^oC)	10^3K (cp-cm^3/g-s)	Density (g/cm^3)	Flowtime (s)	n (cp)
29.50	8.230	1.002	211.4	1.743
39.95	8.183	0.9945	165.6	1.348
50.00	8.138	0.9878	137.4	1.105
55.05	8.114	0.9843	126.1	1.007
60.06	8.090	0.9810	117.5	0.9325
62.55	8.078	0.9793	113.2	0.8955
65.50	8.064	0.9773	110.5	0.8708
67.50	8.055	0.9759	107.4	0.8443
70.00	8.043	0.9743	105.8	0.8291
71.10	8.038	0.9735	104.7	0.8193
72.00	8.034	0.9729	104.9	0.8199
73.00	8.029	0.9722	104.4	0.8149
73.25	8.028	0.9721	103.8	0.8101
73.50	8.026	0.9719	103.9	0.8105
74.10	8.024	0.9715	103.7	0.8084
74.60	8.021	0.9711	103.4	0.8054
74.85	8.020	0.9710	103.2	0.8037
75.05	8.019	0.9710	103.1	0.8028
75.75	8.016	0.9704	102.4	0.7965
76.15	8.014	0.9701	101.9	0.7922
76.35	8.013	0.9700	101.6	0.7897
76.60	8.012	0.9698	101.1	0.7856
77.10	8.009	0.9695	100.2	0.7780
77.45	8.008	0.9692	99.57	0.7728
78.10	8.005	0.9688	97.84	0.7588
79.05	8.000	0.9681	95.46	0.7393
80.05	7,995	0.9675	92.76	0.7175

TABLE XII

Solution #9

X_{H_2O}=0.8061 X_{O_2O}=0.1165 $X_{3\text{-mp}}$=0.0774

Temp (^oC)	10^3K (cp-cm^3/g-s)	Oensity (g/cm^3)	Flowtime (s)	η (cp)
55.00	3.189	0.9839	315.7	0.9905
59.90	3.180	0.9805	295.0	0.9197
65.00	3.170	0.9770	277.3	0.8588
67.45	3.166	0.9753	270.3	0.8345
70.20	3.161	0.9734	267.4	0.8226
71.05	3.159	0.9728	264.7	0.8134
72.05	3.157	0.9721	261.7	0.8031
73.05	3.155	0.9714	259.4	0.7950
74.05	3.153	0.9707	255.9	0.7833
74.50	3.152	0.9704	255.8	0.7825
75.05	3.151	0.9700	254.4	0.7777
75.50	3.151	0.9697	254.2	0.7766
76.00	3.150	0.9694	252.1	0.7697
77.05	3.148	0.9686	248.9	0.7589
78.00	3.146	0.9680	244.3	0.7439
80.05	3.142	0.9666	233.0	0.7076

TABLE XIII

Solution #10

X_{H_2O}=0.9238 X_{D_2O}=0.0000 $X_{3\text{-mp}}$=0.0762

Temp (°C)	10^3K (cp-cm^3/g-s)	Density (g/cm^3)	Flowtime (s)	η (cp)
10.05	9.820	1.007	317.8	3.144
15.00	9.799	1.004	257.2	2.628
19.60	9.779	1.000	227.7	2.228
25.00	9.756	0.9965	194.6	1.892
30.00	9.734	0.9929	171.2	1.655
35.00	9.713	0.9893	151.5	1.456
40.00	9.691	0.9857	135.8	1.297
45.05	9.669	0.9821	122.1	1.159
50.00	9.648	0.9785	112.4	1.061
55.00	9.627	0.9749	102.2	0.9591
60.00	9.605	0.9713	94.65	0.8830
65.05	9.549	0.9676	87.49	0.8084
70.05	9.493	0.9640	80.81	0.7395
75.05	9.438	0.9604	75.28	0.6823
80.05	9.382	0.9568	70.41	0.6321
85.00	9.328	0.9532	64.99	0.5778
89.90	9.273	0.9497	60.58	0.5335

TABLE XIV

Solution #1

X_{H_2O}=0.0000 X_{O_2O}=0.9160 $X_{3\text{-mp}}$=0.0840

Data for Figures 9 and 22

Temp (°C)	LCST = 37.35°C $10^4\varepsilon$	η/η_o	LCST=37.36°C $10^4\varepsilon$	$\varepsilon^{-1}(\eta/\eta_o)^{-25}$
30.00	236.7	1.003	237.0	39.15
31.00	204.5	1.007	204.8	41.01
32.00	172.3	1.011	172.6	44.07
33.00	140.1	1.018	140.4	45.60
34.00	107.9	1.025	108.2	49.85
35.00	75.68	1.038	76.00	51.79
36.00	43.48	1.062	43.80	50.75
36.50	27.38	1.081	27.70	51.51
36.70	20.93	1.086	21.26	59.80
36.80	17.71	1.095	18.03	57.37
36.90	14.49	1.102	14.81	59.55
37.00	11.27	1.112	11.59	60.72
37.10	8.052	1.125	8.373	62.85
37.20	4.831	1.147	5.153	62.93
37.30	1.161	1.192	1.932	64.13

TABLE XV

Solution #2

X_{H_2O}=0.3914 X_{O_2O}=0.5279 $X_{3\text{-mp}}$=0.0807

Data for Figures 10 and 23

Temp (^oC)	$10^4\varepsilon$	η/η_o	$10^4\varepsilon$	$\varepsilon^{-1}(\eta/\eta_o)^{-25}$
	LCST = 48.50^oC			LCST = 48.46^oC
40.00	264.3	1.025	263.1	20.51
41.00	233.2	1.028	232.0	21.62
42.00	202.1	1.030	200.9	23.78
43.00	171.0	1.033	169.8	26.16
44.00	139.9	1.040	138.7	27.05
45.00	108.8	1.051	107.6	26.80
46.00	77.82	1.071	76.49	23.53
47.00	46.63	1.090	45.40	25.55
47.50	31.09	1.112	29.85	23.57
47.60	27.98	1.119	26.74	22.49
47.80	21.76	1.138	20.52	19.24
47.85	20.21	1.131	18.97	24.29
47.90	18.65	1.140	17.41	21.70
48.00	15.54	1.149	14.30	21.71
48.10	12.44	1.162	11.19	20.94
48.20	9.327	1.189	8.084	16.32
48.30	6.218	1.212	4.975	16.43
48.40	3.109	1.243	1.866	23.30

TABLE XVI

Solution #3

X_{H_2O}=0.7356 X_{D_2O}=0.1866 $X_{3\text{-mp}}$=0.0778

Data for Figures 11 and 24

LCST = 64.00°C LCST = 64.00°C

Temp (°C)	$10^4\varepsilon$	η/η_o	$10^4\varepsilon$	$\varepsilon^{-1}(\eta/\eta_o)^{-25}$
30.00	1008.0	1.000	1008.0	9.916
35.05	858.7	1.006	858.7	10.03
39.95	713.3	1.017	713.3	9.198
45.00	563.5	1.029	563.5	8.683
49.90	418.2	1.045	418.2	7.956
55.00	266.9	1.066	266.9	7.580
58.00	178.0	1.085	178.0	7.310
59.00	148.3	1.092	148.3	7.469
60.10	115.7	1.109	115.7	6.508
61.00	88.98	1.123	88.98	6.183
61.95	60.80	1.142	60.80	5.959
63.00	29.66	1.185	29.66	4.840
63.10	26.69	1.194	26.69	4.451
63.15	25.21	1.200	25.21	4.158
63.20	23.73	1.197	23.73	4.703
63.30	20.76	1.206	20.76	4.457
63.40	17.80	1.220	17.80	3.897
63.50	14.83	1.230	14.83	3.813
63.65	10.38	1.247	10.38	3.865
63.70	8.898	1.257	8.898	3.692

TABLE XVII

Solution #4

X_{H_2O}=0.7926 X_{D_2O}=0.1298 $X_{3\text{-mp}}$=0.0776

Data for Figures 12 and 25

LCST = 74.00°C			LCST = 74.00°C	
Temp (°C)	$10^4\varepsilon$	η/η_o	$10^4\varepsilon$	$\varepsilon^{-1}(\eta/\eta_o)^{-25}$
40.00	979.4	1.015	979.4	7.767
45.00	835.4	1.020	835.4	6.301
50.00	691.3	1.035	691.3	6.121
55.00	547.3	1.049	547.3	6.079
60.00	403.3	1.074	403.3	4.260
65.00	259.3	1.108	259.3	2.970
68.00	172.8	1.135	172.8	2.495
69.00	144.0	1.145	144.0	2.404
69.95	116.7	1.159	116.7	2.143
71.00	86.42	1.179	86.42	1.968
71.50	72.01	1.192	72.01	1.794
71.70	66.25	1.197	66.25	1.756
71.95	59.03	1.205	59.03	1.668
72.18	52.43	1.215	52.53	1.527
72.30	48.97	1.217	48.97	1.537
72.48	43.79	1.225	43.79	1.459
72.58	40.90	1.229	40.90	1.440
72.62	39.75	1.231	39.75	1.422
72.68	38.02	1.237	38.02	1.290
72.71	37.16	1.237	37.16	1.347

TABLE XVIII

Solution #5

X_{H_2O}=0.7880 X_{D_2O}=0.1290 $X_{3\text{-mp}}$=0.0830

Data for Figures 13 and 26

LCST = 75.50°C UCST = 77.50°C			LCST = 75.50°C UCST = 77.50°C	
Temp (°C)	$10^4\varepsilon$	η/η_o	$10^4\varepsilon$	$\varepsilon^{-1}(\eta/\eta_o)^{-25}$
40.00	1018.0	1.016	1018.0	6.604
44.98	875.4	1.023	875.4	6.470
50.00	731.4	1.034	731.4	5.927
55.00	588.0	1.051	588.0	4.904
60.00	444.6	1.069	444.6	4.242
62.50	372.5	1.086	372.5	3.410
65.00	301.2	1.101	301.2	2.996
67.50	229.5	1.122	229.5	2.452
70.00	157.8	1.151	157.8	1.884
72.00	100.4	1.189	100.4	1.315
72.50	86.05	1.202	86.05	1.169
73.00	71.71	1.217	71.71	1.028
73.55	55.93	1.233	55.93	0.9512
74.00	43.02	1.249	43.02	0.8959
74.35	32.98	1.261	32.98	0.9202
74.60	25.81	1.276	25.81	0.8749
74.70	22.95	1.277	22.95	0.9648
74.80	20.08	1.279	20.08	1.060
78.85	38.50	1.258	38.50	0.8366
79.10	45.63	1.249	45.63	0.8447
79.50	57.04	1.237	57.04	0.8602
80.00	71.30	1.218	71.30	1.013
80.50	85.56	1.199	85.56	1.251
81.00	99.81	1.192	99.81	1.241
82.00	128.3	1.162	128.3	1.827
83.00	156.9	1.146	156.9	2.113
84.00	185.4	1.132	185.4	2.431
86.00	242.4	1.111	242.4	2.969
88.00	299.4	1.091	299.4	3.785

TABLE XIX

Solution #6

X_{H_2O}=0.7954 X_{D_2O}=0.1245 $X_{3\text{-mp}}$=0.0801

Data for Figures 16 and 28

T_{DCP} = 76.25°C

Temp (°C)	$10^4\varepsilon$	η/η_o	$\lvert T-76^oC\rvert^2$	$(\eta/\eta_o)^{-25}$
40.15	1033.0	1.019	1285.2	0.6247
44.95	895.8	1.022	964.1	0.5804
50.10	748.4	1.041	670.8	0.3662
54.95	609.6	1.053	443.1	0.2750
60.00	465.1	1.072	256.0	0.1758
62.55	392.1	1.087	180.9	0.1242
65.05	320.5	1.101	119.9	0.0902
67.50	250.4	1.123	72.25	0.0550
70.05	177.4	1.149	35.40	0.0310
71.00	150.3	1.170	25.00	0.0197
71.95	123.1	1.180	16.40	0.0160
73.00	93.02	1.201	9.000	0.0103
73.95	65.83	1.222	4.203	0.0067
74.90	38.64	1.244	1.210	0.0043
75.60	18.60	1.239	0.1600	0.0047
76.00	0.0000	1.246	0.0000	0.0041
76.60	10.02	1.243	0.3600	0.0043
77.00	21.47	1.238	1.000	0.0048
78.00	50.09	1.225	4.000	0.0063
79.00	78.71	1.208	9.000	0.0089
79.95	105.9	1.188	15.60	0.0135

TABLE XX

Solution #7

X_{H_2O}=0.7987 X_{D_2O}=0.1241 $X_{3\text{-mp}}$=0.0773

Data for Figures 17 and 29

T_{DCP} = 76.00°C

Temp (°C)	$10^4\varepsilon$	η/η_o	$\lvert T-76^oC\rvert^2$	$(\eta/\eta_o)^{-25}$
40.00	1031.0	1.018	1296.0	0.6402
44.90	890.7	1.022	967.2	0.5804
45.00	887.9	1.020	961.0	0.6095
50.00	744.7	1.037	676.0	0.4032
55.00	601.5	1.050	441.0	0.2953
59.90	461.1	1.071	256.0	0.1800
64.90	317.9	1.097	123.2	0.0988
65.00	315.1	1.100	121.0	0.0923
70.00	171.8	1.143	36.00	0.0354
71.00	143.2	1.153	25.00	0.0285
72.00	114.6	1.170	16.00	0.0197
73.00	85.92	1.182	9.000	0.0153
74.00	57.28	1.194	4.000	0.0119
75.00	28.64	1.206	1.000	0.0093
75.45	15.75	1.208	0.3025	0.0089
76.00	0.0000	1.210	0.0000	0.0085
77.00	28.64	1.203	1.000	0.0098
79.00	85.92	1.181	9.000	0.0156

TABLE XXI

Solution #8

X_{H_2O}=0.8020 X_{O_2O}=0.1207 $X_{3\text{-mp}}$=0.0772

Data for Figures 18 and 30

T_{OCP} = 76.00°C

Temp (°C)	$10^4\varepsilon$	η/η_o	$\lvert T-76^oC\rvert^2$	$(\eta/\eta_o)^{-25}$
39.95	1045.0	1.011	1332.0	0.7607
50.00	744.7	1.041	676.0	0.3662
55.05	600.0	1.053	438.9	0.2750
60.05	456.8	1.076	254.4	0.1602
62.55	385.2	1.082	180.9	0.1394
65.50	300.7	1.111	110.3	0.0720
67.50	243.4	1.115	72.25	0.0658
70.00	171.8	1.144	36.00	0.0346
71.10	140.3	1.151	24.01	0.0297
72.00	114.6	1.170	16.00	0.0197
73.00	85.92	1.182	9.000	0.0153
73.25	78.76	1.180	7.563	0.0160
73.50	71.60	1.185	6.250	0.0144
74.10	54.42	1.194	3.610	0.0119
74.60	40.10	1.199	1.960	0.0107
74.85	32.94	1.201	1.323	0.0103
75.05	27.21	1.204	0.9025	0.0096
75.75	7.160	1.208	0.0625	0.0089
76.15	4.296	1.209	0.0225	0.0087
76.35	10.02	1.217	0.1225	0.0074
76.60	17.18	1.208	0.3600	0.0089
77.10	31.51	1.205	1.210	0.0094
77.45	41.53	1.204	2.103	0.0096
78.10	60.15	1.194	4.410	0.0119
79.05	87.36	1.181	9.303	0.0156
80.05	116.0	1.164	16.40	0.0224

TABLE XXII

Solution #9

X_{H_2O}=0.8061 X_{O_2O}=0.1165 $X_{3\text{-mp}}$=0.0774

Data for Figures 19 and 31

T_{OCP} = 76.45°C

Temp (°C)	$10^4\varepsilon$	η/η_o	$\lvert T-76^oC\rvert^2$	$(\eta/\eta_o)^{-25}$
55.00	613.6	1.040	441.0	0.3751
59.90	473.4	1.063	259.2	0.2171
65.00	327.5	1.091	121.0	0.1133
67.45	257.4	1.107	73.10	0.0788
70.20	178.8	1.144	33.64	0.0346
71.05	154.5	1.148	24.50	0.0317
72.05	125.9	1.152	15.60	0.0291
73.05	97.25	1.160	8.703	0.0245
74.05	68.65	1.161	3.803	0.0239
74.50	55.78	1.169	2.250	0.0202
75.05	40.05	1.172	0.9025	0.0189
75.50	27.17	1.179	0.2500	0.0163
76.00	12.87	1.178	0.0000	0.0166
77.05	17.16	1.181	1.103	0.0156
78.00	44.34	1.175	4.000	0.0177
80.05	103.0	1.153	16.40	0.0285

TABLE XXIII

Solution #10

X_{H_2O}=0.9238 X_{D_2O}=0.0000 $X_{3\text{-mp}}$=0.0762

Data for Figure 20

T_{DCP} = 76.00°C

Temp (°C)	$10^4\varepsilon$	η/η_o	$\lvert T-76^oC\rvert^2$	$(\eta/\eta_o)^{-25}$
35.00	1174.0	1.005	1681.0	0.8828
40.00	1031.0	1.015	1296.0	0.6892
45.05	886.4	1.020	957.9	0.6095
50.00	744.7	1.041	676.0	0.3662
55.00	601.5	1.044	441.0	0.3408
60.00	458.3	1.060	256.0	0.2330
65.05	313.6	1.066	119.9	0.2023
70.05	170.4	1.064	35.40	0.2121
75.05	27.21	1.066	0.9025	0.2023
80.05	116.0	1.068	16.40	0.1931
85.00	257.8	1.051	81.00	0.2884
89.90	398.1	1.041	193.2	0.3662

REFERENCES

1. H. M. J. Boots and A. C. Michels, Physica 103A, 316-324 (1980).
2. R. E. Goldstein and J. S. Walker, J. Chem. Phys. 78, 1506-1508 (1983).
3. J. S. Walker and C. A. Vause, J. Chem. Phys. 79, 2674-2675 (1983).
4. R. E. Goldstein, J. Chem. Phys. 79, 4445-4446 (1983).
5. A. Oeerenberg, J. A. Schouten and N. J. Trappeniers, Physica 103A, 183 (1980).
6. A. R. Kortan, H. V. Känel, R. J. Birgeneau and J. O. Lister, Phys. Rev. Lett. 47, 1206-1209 (1981).
7. J. O. Cox, J. Chem. Soc., pp. 4606-4608 (1952).
8. E. Gulari, B. Chu and O. Woerman, J. Chem. Phys. 73, 2480 (1980).
9. C. M. Knobler and R. L. Scott, J. Chem. Phys. 76, 2606 (1982).
10. T. Ohta, J. Phys. C10, 791 (1977).
11. P. Calmettes, P. Phys. Lett. 39, 1152-1153 (1977).
12. B. Chu, F. J. Schoenes and M. E. Fisher, Phys. Rev. 185, 220-221 (1969).
13. C. M. Sorensen and M. O. Semon, Phys. Rev. A 21, 340 (1980).
14. J. Osman and C. M. Sorensen, J. Chem. Phys. 73, 4142-4144 (1980).
15. J. Osman, M.S. Thesis, Kansas State University, 1981 (unpublished).
16. R. G. Johnston, Ph.O. Thesis, University of Colorado, 1983 (unpublished).
17. K. Ohbayashi and B. Chu, J. Chem. Phys. 68, 5066-5068 (1978).
18. B. Widom, J. Chem. Phys. 46, 3324-3334 (1967).
19. J. C. Wheeler and B. Widom, J. Am. Chem. Soc. 90, 3067-3068 (1968).
20. S. P. Lee, Chem. Phys. Lett. 57, 612-613 (1978).

SHEAR VISCOSITY BEHAVIOR NEAR THE DOUBLE CRITICAL POINT OF THE MIXTURE 3-METHYLPYRIDINE, WATER AND HEAVY WATER

by

GEOFFRY ALAN LARSEN

B.S., Southwest Texas State University, 1981

AN ABSTRACT OF A MASTER'S THESIS

submitted in partial fulfillment of the

requirements for the degree

MASTER OF SCIENCE

Department of Physics

KANSAS STATE UNIVERSITY

Manhattan, Kansas

1984

ABSTRACT

Critical phenomena in binary fluid systems, particularly critical exponents for these systems, have been studied extensively in recent years. Most of these studies have centered on binary mixtures that unmix when cooled below an upper critical solution temperature. We were interested in systems that display what is called reentrant behavior, those that will again mix when cooled below a lower critical solution temperature. We have attempted to answer the question "What is the behavior of the shear viscosity critical exponent as the mixture concentration approaches the double critical point concentration of a system?"

To answer this question, we have measured the shear viscosity as a function of temperature of ternary mixtures of 3-methylpyridine, water (H_2O), and heavy water (D_2O). Because of the relationship between H_2O and D_2O, we believe this is a quasi-binary system. Ten different concentrations, five on each side of the double critical point concentration, were studied. Several of the mixtures were very near the double critical point concentration.

The results were analyzed in two different ways. In the first method, the shear viscosity anomaly is described by

$$\eta/\eta_o = \varepsilon^{-\phi}$$

$$\varepsilon = \frac{|T-T_c|}{T_c}$$

where T_c is the critical temperature being approached and ϕ is the shear viscosity critical exponent. We found the exponent to nearly double as

the double critical point concentration was approached. In the second method, the anomaly is described by

$$\varepsilon^{-1}(\eta/\eta_o)^{-1/\phi_\sim}(\xi^o)^{-1/\nu}+(\xi^o)^{-1/\nu}(\frac{T_c}{\Delta T})\varepsilon$$

for closed-loop systems. ξ^o is a concentration dependent parameter. ν is the correlation length critical exponent. ΔT is the separation between upper and lower critical solution temperatures. The anomaly is described by

$$(\eta/\eta_o)^{-1/\phi_\sim}A^{-1/\nu}(T-T_m)^2+A^{-1/\nu}a(y-y_o)$$

for no-loop systems. A and a are constants. T_m is the double critical point temperature. y_o is the double critical point concentration and y is the concentration of the mixture. The agreement between this analysis and our results was poor for closed-loop mixtures and good for no-loop mixtures.